7-5-2016

A Minor Necessity: Minor Splicing Is Required in Murine Limb Development

Christopher D. Lemoine
University of Connecticut, christopher.lemoine@uconn.edu

A Minor Necessity: Minor Splicing Is Required in Murine Limb Development

Christopher D. Lemoine

B.S., University of Connecticut, 2012

A Thesis
Submitted in Partial Fulfillment of the
Requirements for the Degree of
Master of Science
at the
University of Connecticut
2016

2016

APPROVAL PAGE

Master of Science Thesis

A Minor Necessity: Minor Splicing Is Required in Murine Limb Development

Presented by

Christopher D. Lemoine, B.S

Major Advisor_____
Rahul Kanadia

Associate Advisor_____
Andrew Moiseff

Associate Advisor _____
Joseph Crivello

Associate Advisor _____
David Goldhamer

University of Connecticut

2016

TABLE OF CONTENTS

Abstract

Microcephalic osteodysplastic primordial dwarfism type-1 (MODI) is a rare congenital developmental disorder resulting in patients presenting with microcephaly, limb abnormalities, and growth retardation. This disease, along with the related Roifman Syndrome, results from mutations to the gene *RNU4atac.*[1-3] This gene encodes for the U4atac small nuclear RNA (snRNA) which, along with four other snRNAs (U11, U12, U5, and U6atac) compose the small nuclear ribonucleoprotein (snRNP) complex called the minor spliceosome. Responsible for the excision of a subpopulation of introns (called minor introns), the minor spliceosome is known to play an essential role in eukaryotic limb development.[1-5] However, while mutations in RNU4atac have been shown to decrease efficiency of minor splicing, a direct role of minor splicing in limb development has thus far only been implicated.[2] Utilizing a RNU11 conditional knockout mouse, I demonstrate through a non-U4atac dependent animal model that minor splicing is required for proper development of the murine limb. Using skeletal analysis I reveal that minor splicing results in compromised development of the mouse limb, and that the severity of this developmental disruption increases along the proximodistal axis. Additionally, utilizing TUNEL assays alongside immunofluorescence I demonstrate that that minor splicing may play a role in maintenance of the proliferating progenitor cell population within the developing mouse limb.

Introduction

Microcephalic osteodysplastic primordial dwarfism type 1 (MOPDI) (OMIM 210710), is a rare developmental disorder which has been reported in less than 50 cases world-wide. Individuals born with this disease suffer from severe developmental abnormalities including disruption of brain formation (microcephaly), defects in long bone growth and patterning (osteodysplasia), and general intrauterine growth retardation defined as primordial dwarfism. The prognosis of MOPDI patients is poor, with the majority of confirmed cases dying within their first year of life. In 2011 it was reported that patients suffering from MOPDI possessed either one or multiple mutations in the gene *RNU4ATAC*, which encodes for the U4atac small nuclear RNA (snRNA). U4atac is an essential component of a small nuclear ribonucleoprotein (snRNP) complex called the minor spliceosome.

In all eukaryotes, genes are segmented into coding regions called exons and non-coding regions called introns. In order for these segmented genes to be properly expressed, their initial transcripts must undergo several levels of processing before they can be exported from the nucleus to the cytoplasm. In addition to modifying the transcripts via capping and polyadenylation to allow for transport and prevent degradation, the introns of eukaryotic pre-mRNA transcripts must be spliced out and the exons ligated together. The vast majority of this splicing is accomplished by a snRNP complex known as the major spliceosome. Through the interaction of multiple snRNAs and hundreds of associated proteins, this complex is able to identify the boundaries of introns. It is then capable of binding to specific interacting sites, or consensus sequences, within these introns, and by undergoing a series of structural modifications, conducts two trans-

esterification reactions which simultaneously remove the bound introns and ligate together flanking exons. This mechanism of mRNA splicing is an essential part of eukaryotic RNA processing, and is entirely based around the ability of the major spliceosome to identify specific consensus sequences within the introns. However, there exists a small population of genes which contain introns possessing divergent consensus sequences that cannot be recognized by the major spliceosome complex. These introns must therefore undergo an alternative method of splicing through the use of a unique splicing snRNP complex known as the minor spliceosome.

Alternative splicing allows for a relatively small number of genes (20,000-25,000 in humans) to encode for a much larger range of final protein products (>250,000). Additionally, intron retention can regulate gene expression through pathways such as non-sense mediated decay (NMD). It has been suggested that the lower activity of the minor spliceosome compared to its major counterpart causes inefficient splicing of minor-intron containing genes. Subsequent intron retention could generate a bottleneck, thereby regulating minor intron-containing gene (MIG) expression.[6] While the precise role of minor splicing is not yet known, it has been demonstrated to be required for development in eukaryotes which possess minor introns, including humans.[1-5]

My thesis work seeks to understand what role minor splicing plays in development by investigating how the loss of this cellular process results in limb developmental defects in mice. I propose that minor splicing is required for normal maintenance of progenitor cell populations in the developing limb, and that loss of minor splicing results in a decrease of early progenitor cell populations through a combination of cell death and an exiting of cells from cell cycle. I will utilize a mouse knock-out engineered to conditionally

disrupt expression of the gene *RNU11* which encodes for the U11 snRNA, an essential component of the minor spliceosome. Through a combination of post-natal skeletal comparisons, I will determine if long bone growth is disrupted in mouse limbs lacking U11 expression. I will also use a combination of *In situ* hybridization and immunohistochemistry techniques to investigate whether any difference in the limbs of U11 mutants can be attributed to a shift in progenitor cell proliferation or survival.

RNA Splicing and Minor Splicing

The vast majority of eukaryotic genes are segmented into exonic (coding) and intronic (non-coding) regions. In order for those genes to be expressed and their mRNA transcripts to be accurately translated to a final protein product, the noncoding introns must be removed through a process known as splicing. RNA splicing is the result of interactions between the pre-mRNA transcript and a snRNP complex known as the spliceosome. Most eukaryotic introns undergo splicing by way of the major spliceosome, which consists of five small nuclear RNAs (snRNAs): U1, U2, U4, U5, U6; as well as hundreds of associated proteins. During transcription of the nascent pre-mRNA, the major spliceosome associates with specific consensus sequences within the intron and conducts a series of transesterification reactions which results in the ligation of the 5' and 3' exons and the simultaneous generation and excision of an intron lariat structure (for full review see ref. **7-9**).

The three sites required to direct activity of the major spliceosome are known as the 5'-splice site (5'SS), the branch-point sequence (BPS), and the 3'-splice site (3'SS). These sites consist of characteristic nucleotide sequences and can be annotated as 5'-AG/GTRAGT-3' (where R is a purine), 5'-YUNAY-3' (where Y is C or T), and 5'-NCAG/G-

3’ (where N indicates any nucleotide), respectively.[10-13] The general activity of the major spliceosome is schematized in **Figure 1A**. Splicing begins with the binding of the U1 snRNA and its associated proteins to the 5’SS through complementary base paring of the U1 snRNA and the nascent transcript. The branch point of the intron is then bound by the U2 small nuclear ribonucleoprotein particle (snRNP) through partial complementarity with the U2 snRNA. The major spliceosome complex is completed by the inclusion of a tri-snRNP particle consisting of the U4, U5, and U6 snRNPs. During the splicing process, a specific adenosine residue known as the branch point is displaced due to incomplete complementarity between the BPS and the U2 snRNA. This allows the first transesterification reaction to take place between the branch point adenosine and the 5’SS, forming the intermediate intron lariat structure. RNA splicing concludes with the ligation of the 5’ and 3’ exons through a second transesterification reaction, and the simultaneous release of the intron lariat.[7-9]

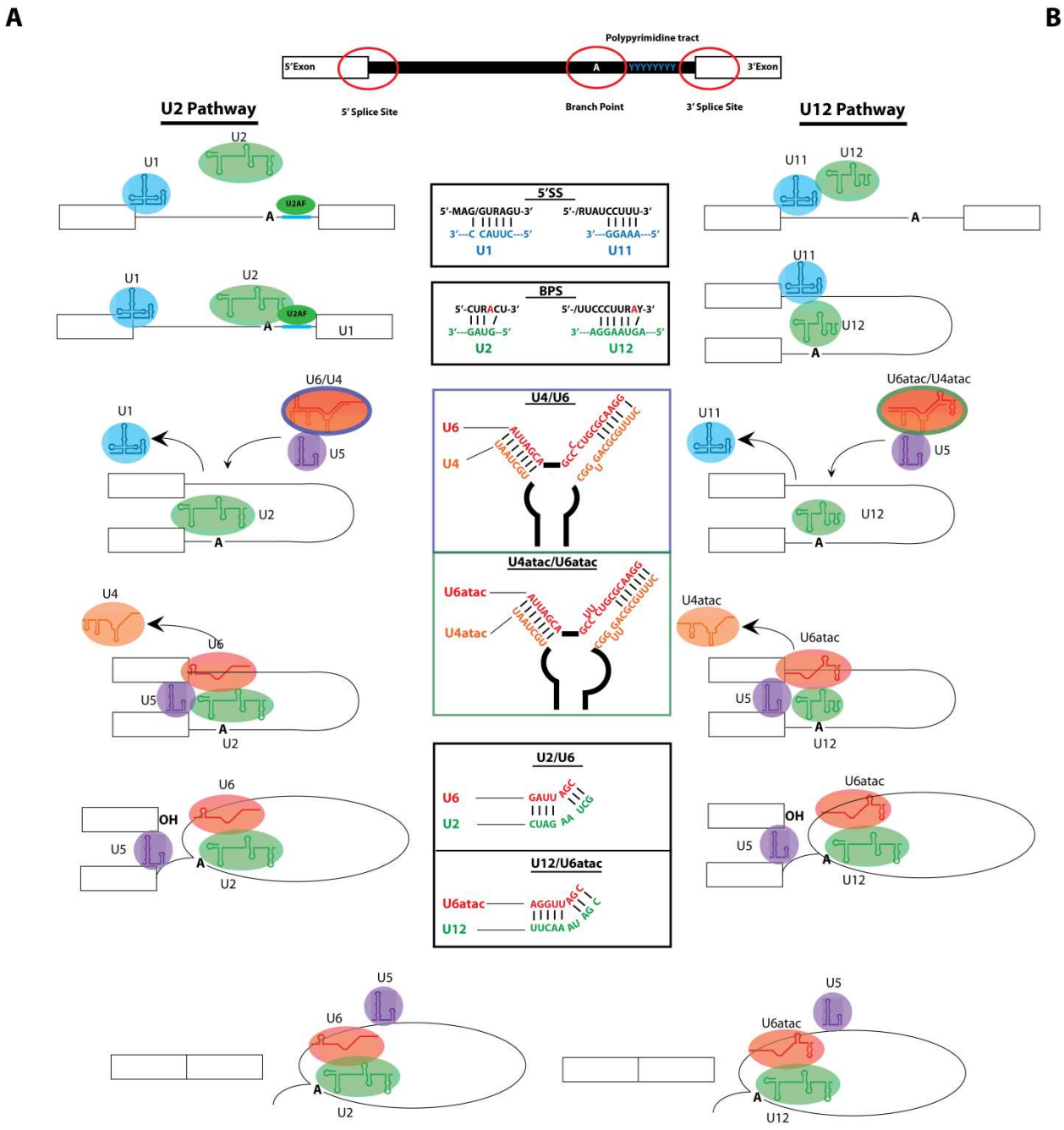

Figure 1: Schematic of eukaryotic mRNA splicing. A) The major splicing pathway and **B)** minor splicing pathways are compared above. Essential RNA-RNA binding regions are diagramed in highlighted boxes comparing how the secondary structures formed are similar in both major and minor splicing. Colored circles indicate splicing snRNP particles while the secondary structures of the major and minor snRNAs are displayed within these circles. Both splicing processes are similar, except in that the U11 and U12 snRNPs of the minor spliceosome bind to their consensus sequences as a di-snRNP, rather than individually as occurs with their major counterparts (U1 and U2).

While major splicing accounts for over 99% of eukaryotic splicing, there exists an extremely small number of introns (<0.5%) which contain consensus sequences that significantly diverge from the majority of introns. The divergence prevents this minor population of introns from being processed by the major spliceosome. A second splicing pathway has therefore evolved to specifically target this intron subpopulation, and was appropriately named the minor spliceosome. Consisting of four unique snRNAs called U11, U12, U4atac, and U6atac, the minor spliceosome also contains the U5 snRNP which it shares with the major spliceosome. The 5'SS, BPS, and 3'SS of minor introns can be described as 5'-/(R)TATCCTTT-3', 5'-TTCCTTRAY-3', and 5'-YAG/-3' respectively.[10,12,14] However, despite their divergence from the consensus sequences of major introns, processing of minor introns by the minor spliceosome is very similar to that of its major counterpart, and is schematized in **Figure 1B**. While the biomechanical processes between the major and minor splicing pathways are similar, a major difference is the fact that unlike U1 and U2, U11 and U12 of the minor splicing pathway exist as a di-snRNP particle, requiring simultaneous targeting of the 5'SS and BPS.

Despite the fact that minor introns compose such a small part of the overall intron population, they are conserved amongst eukaryotes and have been identified in every major eukaryotic super group.[15,16] The extensive proliferation of this intron subpopulation throughout the Eukaryota domain suggests that minor splicing emerged early on during eukaryotic evolution. Despite the rarity of minor introns, loss of minor splicing can have severe developmental repercussions in a wide variety of organisms, giving insight as to the reason for its retention throughout evolution.

Research conducted by Kim et al. in the plant *Arabidopsis thaliana* found that when minor splicing was disrupted, plants were either aborted early in development in knock-out mutants, or else suffered severe developmental defects in knock-down experiments.[4] Additional studies in *Arabidopsis*, *Drosophila melanogaster* and *Danio rerio* have yielded similar results demonstrating that minor splicing is essential for development in almost all eukaryotes, including humans.[1-3,5,17-18]

Since its initial identification as a minor splicing-associated disease, it has been found that individuals with MOPDI suffer from both characteristic CNS developmental defects, as well as a great deal of skeletal malformations including platyspondyly, short iliac wings, short and flat long bones, and flat/irregular acetabular roofs.[19,20] With the identification of *RNU4atac* mutations as the cause of this disease, two groups identified over seven different mutations capable of resulting in this disease (**figure 2**). Splicing assays focusing on these identified mutations demonstrated that disruption to U4atac could result in over a 90% reduction of minor splicing efficiency. Such results for the first time allowed the inference that minor splicing could play an essential role in human development.[1,2]

More recently, disruption of minor splicing has been implicated in another human developmental disease, known as Roifman syndrome (OMIM 616651). In 2015, Merico et al. demonstrated that patients suffering from this congenital disorder also possessed mutations in the *RNU4atac* gene (**figure 2**).[3] Classified as a separate disorder from MOPDI, Roifman syndrome is characterized by several distinct features including antibody deficiency and retinal dysplasia.[21-24] However, both MOPDI and Roifman syndrome share several symptoms including disrupted cognitive development, growth retardation, and skeletal dysplasia.[3,21-24] While it is curious that mutations in the same gene can result in completely separate diseases, the fact that specific developmental defects are at least partially shared between both MOPDI and Roifman patients is informative. In particular, the shared cognitive delays and osteodysplasia common across in both of these diseases indicate that minor splicing plays an essential role in both CNS and skeletal development. While work has already been conducted focusing on the role

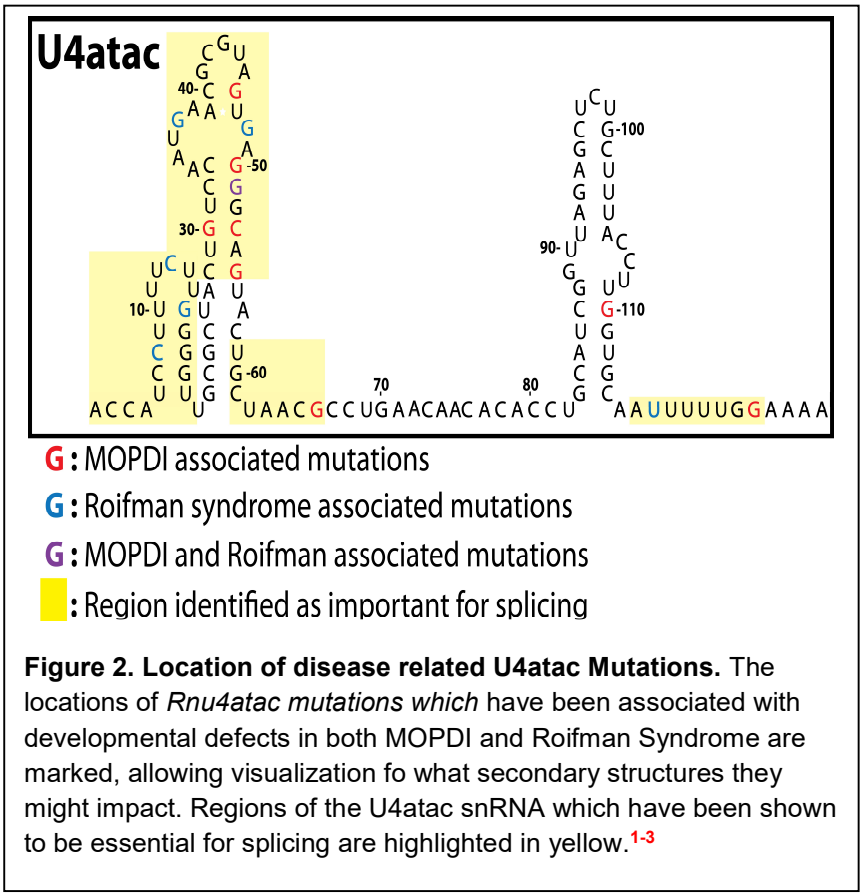

Figure 2. Location of disease related U4atac Mutations. The locations of *Rnu4atac mutations which* have been associated with developmental defects in both MOPDI and Roifman Syndrome are marked, allowing visualization fo what secondary structures they might impact. Regions of the U4atac snRNA which have been shown to be essential for splicing are highlighted in yellow.[1-3]

of minor splicing in brain development, its function in the development of the skeletal system (particularly in regards to limb growth) has yet to be investigated.[25]

The Limb as a Model System

The limb has long been used as a paradigm for studying organogenesis and patterning during development. As a system, the limb allows for the simultaneous study of multiple tissue types including muscle, nervous, and bone. Additionally, unlike other systems, in many animals limbs are not essential for embryonic survivability. As such, major or even complete disruption of the limb through either genetic or mechanical manipulation will not cause death during gestation, thus allowing for thorough investigation of the initiation of its growth throughout development.

Development of the limbs in mice is staggered, with growth of the forelimb initiated at embryonic day 9.5 (E9.5) and hindlimb growth beginning approximately a half day later at E10.[26] Limb development starts with the expansion of the mesenchyme tissue within the **lateral plate mesoderm** (LPM). This expansion occurs only at specified regions along the anterior-posterior axis of the developing embryo, known as the limb field. In mice, these limb fields are found adjacent to specific somite ranges with fore- and hindlimbs forming between somites 13-17 and 27-31, respectively.[27] After the initiation of growth at these pre-specified positions, the limb itself develops rapidly with the three skeletal domains of the limb (stylopod, zeugopod, and autopod) finishing their patterning by the end of E14 (**figure 3A**).

Before growth of the limb can occur, the limb fields must first be established at the specified somite regions. While the precise signals involved in this limb field preparation

are still under investigation, it has been suggested that limb field establishment relies on expression of **retinoic acid** (RA) from within the trunk mesoderm. This role of RA was initially proposed due to investigations in chicks which found that insertion of RA-soaked beads could result in the initiation of ectopic limb growth.[28] Further studies confirmed that if RA synthesis was disrupted by way of Disulphiram addition prior to limb outgrowth, loss of RA was capable of abolishing limb development.[29] The possibility of RA acting as the direct effector of limb bud initiation is unlikely. While mouse knockouts of retinaldehyde dehydrogenase 2 (*raldh2*), the enzyme responsible for RA synthesis, do result in failed initiation of forelimb development; rescued limb development through a low RA diet displayed no RA in the LPM. This would indicate that while RA is essential for limb development, it is likely the initial role of RA lies in establishing the limb field, rather than in the initiation of limb growth.[30-32]

Once the limb fields have been established the first stage of limb growth is the formation of the limb bud, a small ectodermal sack which encompasses the proliferating mesenchymal tissue. Formation of this bud is driven by additional signals from the LPM, believed to consist primarily of **fibroblast growth factors** (FGFs). FGF10, a paracrine factor secreted by mesenchymal cells of the LPM, is thought to be the most likely candidate for initiation of limb bud growth from the established limb field. Whole-mount *in situ* hybridization of FGF10 in chicks has revealed that FGF10 is initially expressed throughout the LPM before becoming restricted to the prospective limb mesoderm and eventually the limb mesenchyme.[33] Additionally, ectopic expression through FGF10 soaked beads results in initiation of ectopic limb growth by inducing FGF8 expression in the overlying ectoderm.[34]

After the initial induction of the limb bud, the mesenchyme cells of the limb establish an essential signaling center in the overlying ectodermal tissue called the **apical ectodermal ridge** (AER). The induction of this ectodermal signaling center is believed to be the result of interactions between Wnt/β-Catenin and FGF10. Within the mesenchyme of the limb bud, Wnt/β-Catenin signaling is required for expression of FGF10. This was demonstrated through the implantation of cells engineered to express Wnt-2b into chick mesenchyme. The implanted cells were capable of causing FGF10 expression within the mesenchyme, eventually resulting in the formation of ectopic limbs.[35] FGF10 derived in the limb bud mesenchyme is capable of inducing expression of FGF8 in the overlying ectoderm. This induction has been demonstrated through misimpression experiments in the chick to act through an intermediary of Wnt3a.[36] FGF8 produced from the now formed AER is then capable of inducing continued FGF10 expression within the limb bud mesenchyme, generating a feedback loop which assists in maintaining a functioning AER.[35-38]

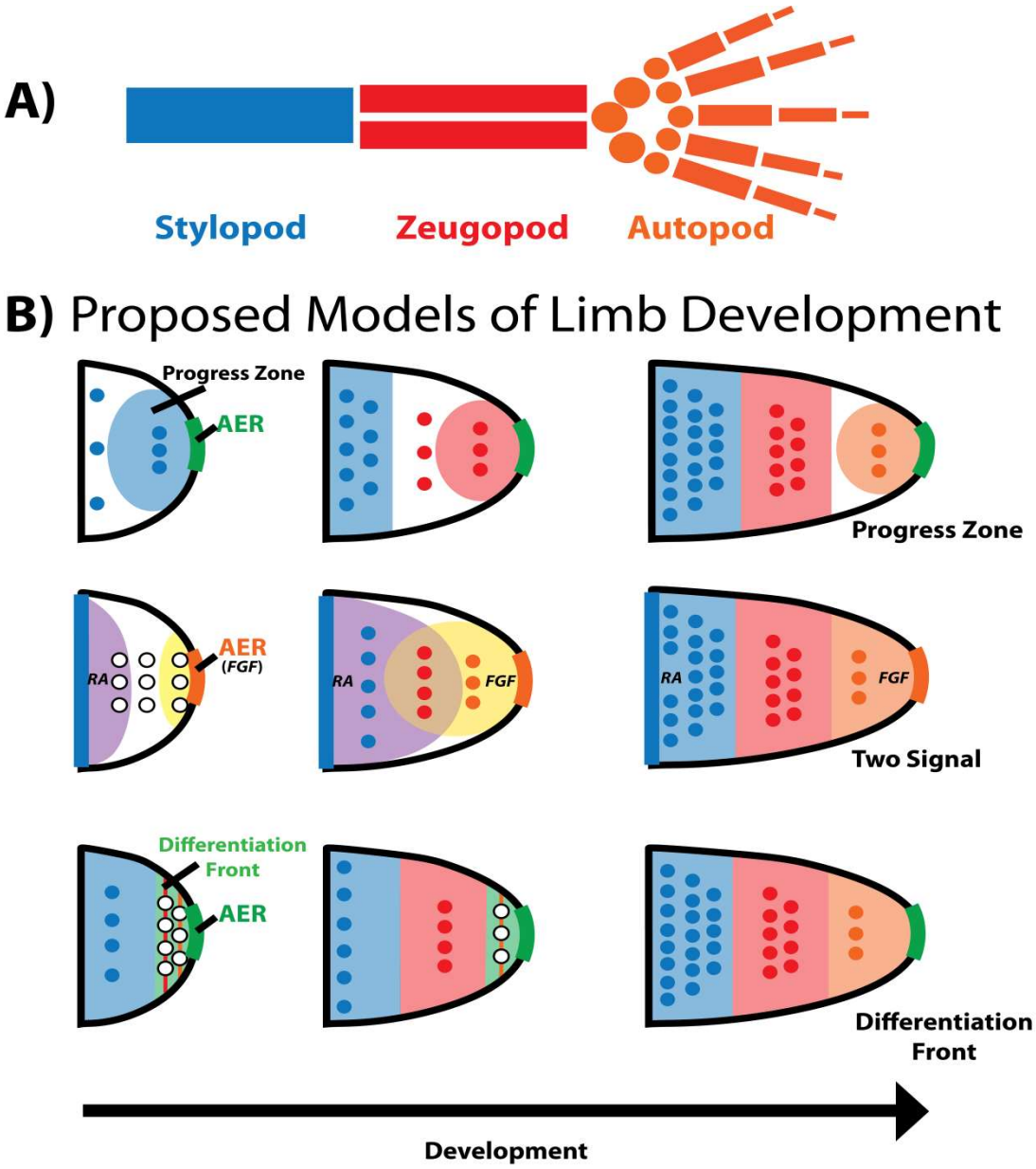

Figure 3: Refinement of limb developmental models. A) The skeletal elements of the mouse limb. The stylopod region contains the proximal long bone (humerus, femur), while the zeugopod forms the distal long bones (radius/ulna, tibia/fibula) and the autopod generates the wrist (carpals, tarsals), palm (metacarpals, metatarsals, and digits (phalanges). **B)** The **progress zone model** sought to explain the results of AER removal experiments conducted in the chicken limb bud. It was hypothesized that the AER acts as a time-keeping mechanism, dictating proximal to distal cell fate (colored regions) of the underlying mesenchymal cells based on duration of exposure to AER signaling within the progress zone (the labeled circular region). **C)** Molecular analysis of the developing limb bud gave rise to the **Two Signal model** of development . This model proposes that early in development the proximal region of the limb is patterned by retinoic acid (RA) expression while the distal regions are specified by exposure to FGF signaling from the AER. Mesenchyme receiving input from both signaling regions forms the interior zeugopod region. D) The **differentiation front model** attempted to reconcile earlier proposed concepts of limb patterning. This model suggests that patterning of proximal to distal regions are set early in development, but progenitor cells are kept in an undifferentiated state as long as the within the differentiation front. Exiting of this region causes differentiation and allows for the expansion of the already specified limb regions.

With the establishment of the limb bud, proximal-distal growth as well as anterior-posterior patterning within the limb is driven by a complex network of signals between multiple regions within the limb itself (**figure 3**). Several models have been proposed to describe limb growth beginning with early seminal work by Saunders in 1948. Using chicken embryos, Saunders removed the most distal region of the developing chick limbs at progressively later time points. It was found that earlier removal of this region (containing the AER) would result in more proximal disruption of limb growth.[39] Building off of these experiments Wolpert et al. proposed the **progress zone** model of limb development (**figure 3B**). Postulating a time-keeping role for the AER, the progress zone model of limb growth suggests that signals secreted from the AER maintain the proliferative ability of mesenchyme cells in the distal end of the developing limb known as the "progress zone." Cells which lie within this zone of influence are allowed to proliferate while remaining in an undifferentiated state. Their eventual proximal-distal fate is determined temporally, based on what time in development they exit the migrating progress zone. Those cells which leave the AER's influence early become components of proximal structures (scapula/pelvis, humerus/femur) while those which travel within the zone until later in development take on more distal identities (ulna/tibia, radius/fibula).[39,40] While this model succeeded in describing the results of AER removal experiments, the progress zone cannot be easily reconciled with more recent genetic experiments.

In the investigation of the AER signaling in limb development, it has been shown that loss of the AER can be rescued through expression of FGF molecules, identifying them as the primary signaling molecules of the AER (AER-FGFs).[41-44] While four of these FGF signaling molecules have been found to be expressed specifically in the AER (FGF4,

FGF8, FGF9, and FGF17), FGF8 is both the earliest present, as well as the only FGF expressed throughout the entirety of the AER.[45-48] When a knockout mouse lacking FGF8 was generated, limb growth of these mice was severely stunted, and proximal skeletal elements failed to form correctly.[49] Additional genetic analysis and fate mapping experiments by groups such as Mariani et al. and Dudley et al. have shown through a combination of genetic analyses and fate mapping that the proximal-distal axis of the developing limb is laid out early on in development. Additionally, these specified progenitor pools expand sequentially in proximal to distal direction.[48,50] Observations such as these run counter to the proposal that the AER plays a permissive time-keeping role in development. Instead these experiments seemed to suggest a far more active role for the AER in proximal-distal patterning; necessitating a new model for limb development.

Work conducted using the chick limb has given some evidence that retinoic acid is capable of informing proximal identity in the developing limb.[51]In addition, the same experiments which demonstrated the necessity of updating the progress zone model have given strong evidence to the role which FGF8 and the AER play in establishing proximal-distal limb identity.[48] The two signal/early specification model proposes that the antagonistic signaling between RA and AER-FGFs results in the establishment of the proximal-distal axis of the limb (**figure 3C**). This model in turn coincides with the mapping of specific transcription factors correlating to specified regions of the developed limb. Retinoic acid induces expression of *Meis1* and *Meis2* within the stylopod region while FGFs from the AER result in expression of homeobox A11 and A13 (*Hoxa11*/*Hoxa13*) in the more distal regions of the zeugopod and autopod fated cells.[51,52] While this two-signal system works to reconcile the early specification problem found in the progress zone

model, it too requires further modification. In particular, RAs role as both the initiator of limb bud growth as well as the establishing factor of proximal cell fate is a matter of continued further study. Loss of retinaldehyde dehydrogenase 2 (Raldh2), an enzyme required for RA synthesis in mice, leads to disruption of the initiation of limb bud growth. This effect can be rescued by the application of exogenous retinoic acid, giving support to its role in establishing the prospective limb field.[30] However in studies conducted on mice in which the limb bud initiation was rescued using RA, it was shown that RA signaling may take place through inhibition of FGF8 (an AER-FGF) in proximal mesenchyme rather than through RA acting as a polarizing factor itself.[32]

In an attempt to reconcile the aforementioned models in 2007 Tabin proposed the **differentiation front** model (**figure 3D**). This model proposes that the mesenchyme of the early limb bud is pre-specified to form proximal structures of the limb. However, this proximal "default" can be modified by FGF signaling from the AER which can in turn instill distal cell fates. The FGF signals are able to maintain the underlying distal mesenchyme in an undifferentiated proliferating state. The border region between proximal determined cells and the proliferating mesenchyme is defined as the differentiation front, which continues to move distally as the limb expands.[53]

While the precise model to describe limb patterning and growth is an area of continuing study, several aspects of limb growth have been well investigated, particularly in regards to anterior-posterior patterning in the limb, as well as limb expansion during development. Early work conducted through transplantation experiments of chick limb mesenchyme to ectopic regions of the limb bud revealed the existence of an organizer within the posterior mesenchyme of the developing limb bud.

This organizer, known as the **zone of polarizing activity** (ZPA), was shown to be the primary center of establishing anterior-posterior identity within the limb through the paracrine signaling molecule sonic hedgehog (SHH). Loss of SHH expression through genetic inactivation results in loss of posterior digits while ectopic expression of SHH through transplantation of SHH-expressing cells to the anterior region of the developing limb results in mirror-image digit duplication.[54,55] This paradigm of gradient patterning was described by Wolpert as a **French-flag** model of development wherein AP identity could be determined based on a cell's exposure to a gradation of SHH (**figure 4A**).[56]

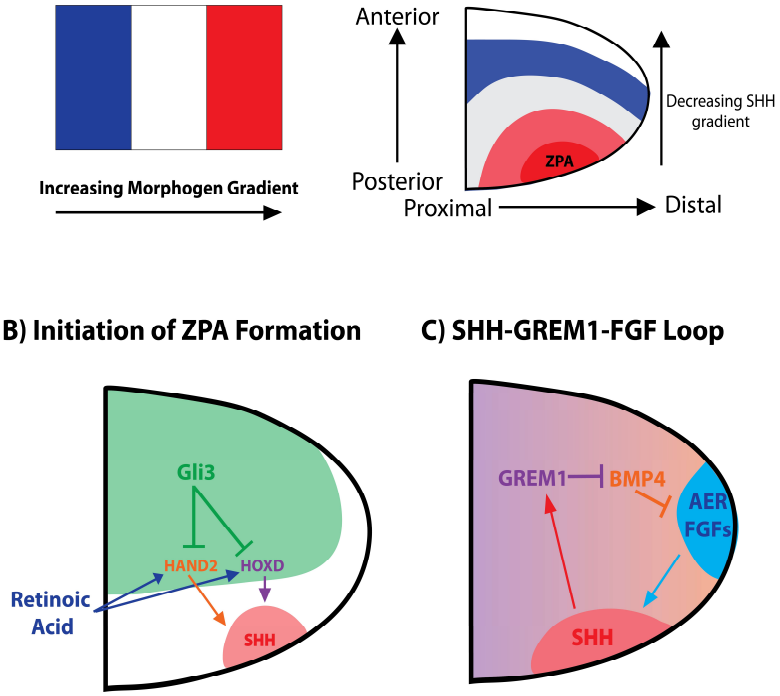

Figure 4. ZPA Formation and Establishment Of SHH-GREM1-FGF feedback Loop. A) The French-flag model of development patterning proposes that a signaling center releases a concentration dependent signaling molecule (a morphogen) which is then capable of establishing a developmental pattern based on the concentration gradient of the molecule. Such a model has been proposed for SHH signaling to induce A-P patterning within the developing limb. **B)** Initiation of the SHH generating ZPA is the result of HAND2 and 'HOXD from the limb mesenchyme. Establishment of HAND2 and HOXD may rely on RA while localization of the ZPA to the posterior limb region results from Gli3 repressor activity. **C)** Maintenance of both the AER and ZPA require a signaling interaction between the two regions. This interaction is mediated by inhibition of BMP4 activity by GREM1 in the limb bud mesenchyme. Shh from the ZPA maintains GREM1 expression. This in turn prevents BMP activity from terminating FGF signaling within the AER, allowing the continued FGF feedback required to maintain the ZPA.

Initiation and localization of the *shh*-expressing ZPA has been shown to be dependent on the interaction between several signaling factors (**figure 4B**). Two of the leading initiators of ZPA formation are believed to the 5'- located Hoxd (*5'HOXD*) and the heart and neural crest derivatives 2 (*HAND2*) genes, the loss of which disrupt shh expression in the developing limb.[57-60] Initiation of these genes is believed to possible rely on RA signaling from the trunk mesoderm, while their restriction to the posterior region of the developing limb bud is carried out by activity of GLI3 activity (**figure 4B**).[30,49,61]

Beyond their roles of anterior-posterior and proximal-distal pattering, the maintenance of both the ZPA and AER are linked to one another in a complex feedback loop. The importance of AER-ZPA interaction was first confirmed by the fact that after AER removal, both continued limb outgrowth and *Shh* expression could be maintained by the application of FGFs.[62,63] A summarized schematic of the SHH-GREM1-FGF signaling loop is schematized in **figure 4C** which displays the interactions between the ectodermal AER, the posterior ZPA, and the mesenchyme of the developing limb itself. Once the AER and ZPA have both been induced the ZPA requires continued FGF input from the AER in order to maintain SHH expression.[62,63] The AER is capable of maintaining this FGF expression by way of an intermediary signaling pathway within the limb mesenchyme consisting of gremlin 1 (GREM1), a bone morphogenetic protein (BMP) antagonist and BMP4. The importance of GREM1 as an intermediary in ZPA-AER signaling was confirmed through inactivation of *gremlin 1* in mice, resulting in both a halt of distal limb bud expansion, as well as disruption to AP pattering.[64] In normal mice SHH is able to maintain GREM1 expression which in turn, through antagonistic action against BMP4, allows for the continued expression of FGF's from the AER. It is this SHH-GREM1-FGF

feedback loop which allows for the continued proximal distal expansion, as well as the AP patterning, of the developing limb.

Taking into account the complexity of the interactions between signaling centers which must occur for proper limb development to take place, it is perhaps not surprising that the limbs are one of the main systems impacted by disruption of minor splicing in MOPDI patients. Is minor splicing required for normal limb development, or is the osteodysplasia observed in patients with mutations in the *U4atac* gene a result of an as-of-yet unidentified disease pathway? Until recently, the 90% reduction in minor splicing efficiency described due to U4atac mutations have only been correlative to diseases such as MOPDI and Roifman Syndrome. Minor splicing itself has not yet been demonstrated to be the direct cause of the limb defects reported in patients with U4atac mutations. However, the recent generation of a U11 conditional knock-out mouse line gives us a novel approach of investigating the direct impact of minor splicing on limb development. With these mice I plan to test whether minor splicing is indeed the direct cause of the limb defects found in MOPDI patients. Additionally, in this thesis I demonstrate that disruption of cell cycle within the proliferating mesenchyme of the developing limb could describe at least some of the symptoms reported in MOPDI and Roifman. Finally, I will seek to describe how minor splicing might fit into currently proposed models of limb development.

Materials and Methods

Mouse Genetics

The Rnu11 conditional knockout mouse used for this project was generated with assistance from the University of Connecticut Health Center. An independent targeting construct was generated for each loxp site flanking the RNU11 on chromosome 4. The 5' loxp site construct was engineered using a PGK-Neo cassette flanked by loxp sites, which was then targeted into 129X1/SvJ mouse embryonic stem (ES) cells. G418-mediated positive selection was used to confirm successful targeting and was followed by negative selection with FIAU. When a positive clone was achieved, removal of the Neo cassette was conducted via transient transfection of cre. The 3' loxp site construct containing a Frt site-flanked PKG-Neo cassette and one loxp site downstream of the 3' Frt site, was targeted into the positive clone. G418 and FIAU were again used to identify clones that underwent successful homologous recombination. This ES cell clone was then injected into C57BL/6 blastocysts to generate a chimaera. Germline transmission and ablation of the Neo cassette was verified by introducing germline Flp recombination. Proper loxp site placement in the resulting mouse line was confirmed by PCR. Prrx1-cre was bred into the $Rnu11^{Fl}/_{Fl}$ to achieve a conditional knockout line to target Rnu11 for removal in the developing limb mesenchyme.

P0 Skeletal Preparations

P0 mouse pups were harvested, anesthetized and euthanized via cooling. Skin and viscera of the pups were removed using forceps. To remove epidermis from paws, carcasses were scalded in $65^{O}C$ water for 45 seconds. Pups were then fixed in 4%

paraformaldehyde overnight at 4^{O}C. After approximately 12hrs pups were then switched to 95% EtOH and allowed to sit overnight at 4^{O}C. Initial cartilage staining was conducted using alcian blue (Sigma A3157) in a solution consisting of 95% EtOH and 25% acetic acid. After initial staining, skeletons were washed in 95% EtOH and treated in 2% KOH for 2-3 days until mostly clear. After KOH clearing, ossified tissue was stained for 1-2 days in a solution of 0.015% Alizarin red (w/v) and 1% KOH. Clearing was conducted in 1% KOH/20% Glycerol for 2 days followed by a final clearings step in 1% KOH until skeleton could be cleanly imaged. After initial imaging skeletons were stored at 4^{O}C in a 1:1 ratio of glycerol and 95% EtOH.

PCR for U11 riboprobe preparation

Mouse tissue was harvested from various developmental stages and the total RNA was collected from the retinal tissue utilizing Tri-Zol as described by the manufacturer. cDNA was then generated from 5µg of the collected RNA. 50 ng of oligo dT primers and 300 ng of hexamers were mixed with total RNA and incubated for 10 minutes at 65^{O}C. The mixture was then set to incubate further for 15 minutes at room temperature. 1µl of reverse transcriptase (Roche), 2.5mM dNTPs, and 1 µl of RNase inhibitor (Roche) were then added to the reaction mix and left to incubate at 42^{O}C for 1 hour. RT-PCR was then conducted utilizing the following primer pairs: forward Rnu11 (5'-AAA GGG CTT CTG TCG TGA GTG GC-3'), reverse Rnu11 (5'-CCG GGA CCA ACG ATC ACC AG-3'). The PCR protocol used for the PCR was 30 cycles of 95^{O}C for 30 seconds, 65^{O}C for 30 seconds, and 72^{O}C for 2 minutes.

pGEMT Cloning and Sequencing

PCR products were visualized on a .9% agarose gels. The agarose gels were mixed with ethidium bromide (EtBr) for visualization of DNA by florescence of EtBr under UV light. The resulting band for U11 coding was excised using razors and isolated by Gel Extraction Kit (Qiagen), using the protocol described by the manufacturer. 1 µl of the gel extraction product was added to a solution containing .5 µl of linearized pGEMT (cut with EcoRI), 1 µl of T4 ligase, 1 µl 10x ligase buffer, and 6.5 µl ultra-pure water. The ligation reaction was then left to incubate at 4^{O}C overnight. 50 µl of DH5-α cells were transformed by adding 3µl of the pGEMT ligation mixture to the cells, and then allowing them to sit on ice for 10 minutes. A 30 second heat shock at 42^{O}C was then administered to the cells before they were allowed to sit on ice once more for 10 minutes. The transformed DH5-α cells were then plated onto LB-AMP. Surviving colonies were then amplified and sent for sequencing.

In situ Probe Preparation

To prepare a probe for mouse in situ hybridization, a pGEMT plasmid containing the U11 sequence was used as a template for PCR amplification using primes complementry to the T7 and Sp6 sites that exist in pGEMT and flank the U11 insert. The linear fragments that resulted from PCR amplification were then seperated on .9% agarose gel, and the band containing U11 was extracted using a Gel Extraction Kit (Qiagen). This gel extrated product was then used as a templae for Sp6 RNA polymerase to generate an antisense riboseprobe. 2 µl of the gel extraction product were combined with 2 µl 10x Sp6 buffer (Roche), 1 µl RNase inhibitor (Roche), 1 µl Sp6 RNA polymerase

(Roche), 2 µl of 10x Nucleotide DIG-labeling Mix (Roche), and 12 µl of DEPC-treated water. The reaction mixture was incubated for 2 hours at 37^{O}C. The transcription reaction was then treated with 1 µl of DNase and left to incubate at 37^{O}C for 15 minutes. The resulting RNA probes were then precipitated using ethanol and resuspended in a mixture containing 10 µl DEPC-treated water and 90 µl DI formamide.

Whole-mount In situ Hybridization

Embryos were harvested at embryonic days 9, 10.5, and 12. Embryos were initially fixed in 4% PFA/PBS overnight at 4^{O}C. After fixing embryos were washed in PPBS mixed with 1% TWEEN (PBT) and dehydrated using a graded methanol/PBT series (25%, 50%, 75%, 100%). Embryos were then stored in 100% methanol until used. For WISH embryos were rehydrated in a 75%, 50%, 25% methanol/PBT series. They were then washed with PBT at room temperature. Bleaching of embryos was conducted in 5% H_2O_2 for 1 hour at room temperature. Embryos were then washed with PBT and treated with proteinase K for 6 to 15 minutes ranging with age of embryo. Proteinase K was inactivated using glycine and embryos were washed before re-fixing in 4% PFA and 0.2% glutaraldehyde in PBT. Final washes were conducted in PBT and the embryos were hybridized with the U11 riboprobe at 70^{O}C overnight. After hybridization embryos were washed several times in SSC solutions to remove unbound probe and blocking was conducted with 10% HISS/0.1% Boerhinger Mannheim blocking reagent in in TBST. Embryos were incubated α-DIG-AP (Roche) at 1:2500 overnight at 4^{O}C. Embryos were then washed in TBST for a day before development using BCIP and NBT.

Section In situ Hybridization

The in situ hybridization of the U11 was performed with 20 μm sections of mice limbs from various developmental time-points. The tissue was fixed using 4% PFA and washed using PBS mixed with .1% TWEEN. The cryosections were then incubated for 10 minutes at room temperature in 1 μg/ml PK (Roche) in PBS. All slides were then acetylated at room temperature for 10 minutes. After words slides were hybridized with 3μl of in situ probe in 150 μl hybe solution overnight at 65^{O}C. The retinal sections were then washed in SCC, treated with RNase A, and incubated with α-DIG-AP (Roche) at 1:2500 concentration in 5% HISS/MABT. The sections were then developed using BCIP and NBT before being mounted using gelvatol.

Immunofluorescence

25 μm cryosections of mice limbs were hydrated in PBS at room temperature before being blocked for 1 hour at room temperature using a blocking buffer consisting of 0.2% BSA, 0.1% Triton-X 100, and 0.02% SDS in PBS. These limb sections were then incubated at 4^{O}C in primary antibodies diluted in blocking buffer. The primary antibodies used for E14, E12, and E11 were mouse anti-Ki67 (1-300 dilution), rabbit anti-Ph3 (1-300 dilution), and Rabbit anti-Sox9 (1-300 dilution). The following day cryosections were washed with blocking buffer for 3 hours with changes in buffer every 10 minutes. They were then incubated overnight at 4^{O}C with secondary antibodies of either Donkey anti-mouse, or donkey anti-rabbit (1-500 dilution). The final day sections were washed with blocking buffer for 3 hours with changes in buffer every 15 minutes. DAPI was added to the blocking buffer for E12 electroporation sections to stain cell nuclei. All sections were

then washed three times with PBS and mounted using ProLong Gold Antifade reagent before being imaged using confocal microscopy.

Results

U11 is expressed in developing limbs and is lost in Prrx1-cre driven cKO

To confirm that the minor splicing snRNA U11 is indeed expressed in MOPDI and Roifman syndrome affected tissue, whole mount *In situ* hybridization (WISH) was conducted using a RNA probe complimentary to U11. At E9 growth of the forelimb has just initiated and as development of the hindlimb is delayed by half a day, it is not yet visible. At this time, alkaline phosphatase (AP) staining demonstrates that U11 is expressed throughout the majority of the developing embryo, except noticeably the heart. By the point in development, both the developing CNS and the forelimb bud have high levels of *Rnu11* expression (**figure 5A**). By embryonic day 10 both the fore- and hindlimb are clearly present, with U11 expression visible in both

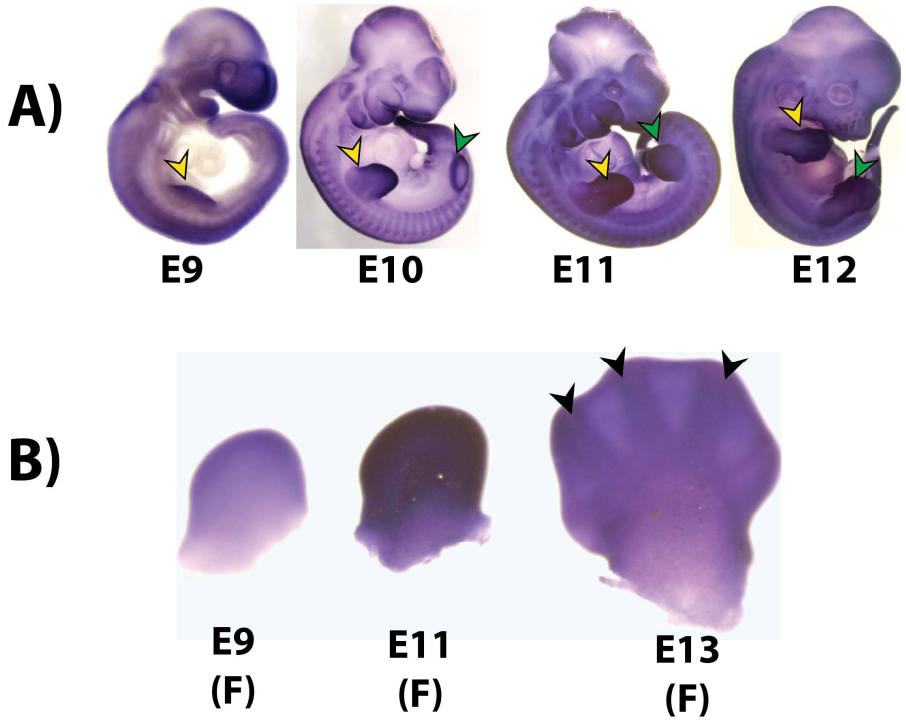

Figure 5: U11 Whole-Mount *In Situ* Hybridization. A) Alkaline phosphatase staining shows localization of U11 expression within the developing embryo at varying time points in limb development. Yellow arrows mark forelimb outgrowth. Green arrows mark hindlimb outgrowth. AP staining demonstrates U11 is expressed in both limbs throughout development. **B)** Closer inspection of the forelimb bud shows that U11 is expressed throughout the limb, and expression increases by E11. At E13 U11 expression can be seen through the entire limb. Arrows indicate cartilage condensations' which will give rise to boney elements of the digits.

of the developing limb buds. This expression continues into E11 where the limbs are perhaps the most highly expressing region of *Rnu11*. By E12 the limb paddle has completely formed with both limbs continuing to demonstrate high levels of U11. In the limb bud itself, AP staining appears uniform throughout from E9 to E11. By E13, U11 expression can be seen in the entirety of the limb paddle, including the mesenchyme condensations which will eventually form the digits of the autopod (**figure 5B**).

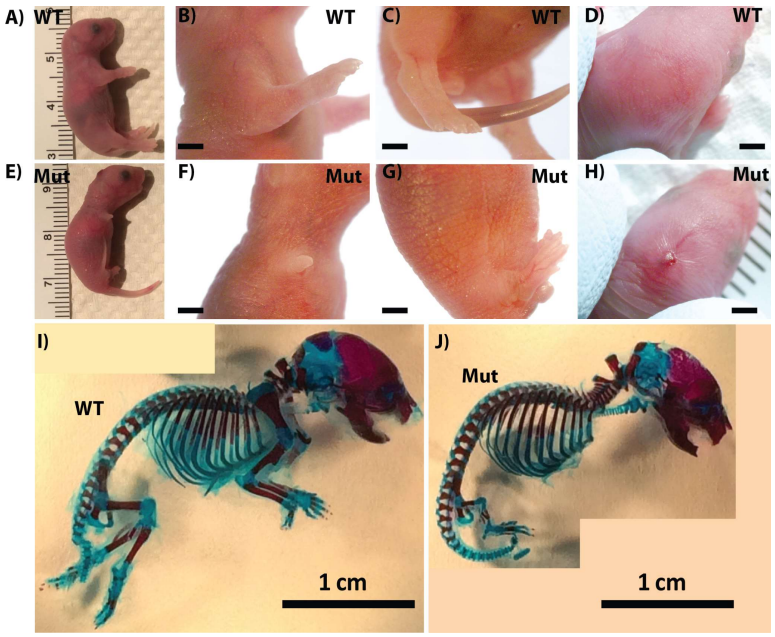

Figure 6: Gross Phenotype of U11 cKO Mutants. A/E) Full-body comparison of wild-type P0 pup and U11 cKO littermate. Severe disruption of development can be observed in both fore- and hindlimb regions. **B/F)** Magnified image of wild-type and mutant forelimb reveals complete loss of gross anatomical structure in P0 mutant. **C/G)** Comparison of wild-type and cKO hindlimb reveals that while there is a decrease in overall size of the mutant hindlimb, patterning appears patterning appears unaffected. P0 mutant hindlimb. **D/H)** P0 U11 cKO mice develop an encephalocele, likely due to Prrx1-driven loss of U11 in the craniofacial mesenchyme. **I/J)** Skeletal staining was conducted to analyze how loss of U11 in the limb bud mesenchyme impacted skeletal development by P0. Alcian blue (blue stain) was used to stain cartilage while alizarin red (red stain) was employed to mark calcium, allowing for identification of ossifying bony elements.

Loss of U11 Results in Major Disruption of Mouse Limb Development by P0

To generate a limb specific Rnu11 cKO mouse, *Rnu11*$^{Wt/Fl}$::Prrx1-cre mice were crossed with *Rnu11*$^{Fl/Fl}$. This cross resulted in mutants easily discernable from wild-type littermates due to major disruption of both the fore- and hindlimbs (**figure 6A/E**). Though

limb development was impacted, all mutant pups were born alive and have survived up to post-natal day 6 (data not shown). In addition to limb defects, mutants were born with an encephalocele in the posterior region of the skull, likely a result of Prrx1-driven U11 loss in craniofacial mesenchyme (**figure 6D/H**).

Disruption of limb development at P0 is most severe in the forelimb. In both wild-type and mutant pups, the stylopod cannot be viewed as it develops internally. However, while the zeugopod and autopod are clearly identifiable in wild-type littermates, no zeugopod or autopod regions were discernable in mutants. The only gross anatomical structure visible was a small stump in the location of the forelimb. While it is possible that this structure could represent either an undeveloped zeugopod or autopod, there are no signs of individual digits that would allow for confirmation of this identification (**figure 6B/F**). The hindlimbs of these mutants appear to be fully patterned with the zeugopod and autopod identifiable in both wild-type and mutant pups (**figure 6C/G**). However, a severe difference in size between wild-type and mutant hindlimbs demonstrates that development is clearly influenced by loss of U11.

To more accurately determine what skeletal defects might give rise to the phenotype observed, I conducted skeletal preparations of both wild-type and mutant pups at P0. Alcian blue was employed to stain acidic polysaccharides allowing for the visualization of cartilage through the staining of glycosaminoglycans. In addition, Alizarin red was used to identify calcium containing tissue, allowing for visualization of ossifying bone (**figure 6I/J**).

Staining of P0 WT skeletons reveal a fully patterned forelimb. When the surrounding connective tissue has been cleared, the stylopod, zeugopod, and autopod of

these mice are all evident. All three forelimb long bones (humerus, ulna, and radius) consist of a central diaphysis identifiable due to alizarin red staining, flanked by two alcian blue stain epiphyseal regions consisting of non-ossified cartilage (**figure 7**). Though stunted, development of forelimb boney regions does occur in mutants. Skeletal preparation revealed that a partially formed scapula was present in 100% of mutants (**figure 7A**). Articulating to this scapula, all mutant forelimbs possess the most proximal long bone: the humerus (**figure 7B/D**). Sequential to the humerus in mutants is what appears to be a single distal long bone, believed to likely be the ulna (**figure 7C/E**). The most distal regions of the limb, primarily the skeletal components of the autopod, appear to be subject to a high degree of variability in their disruption. While skeletal preparation revealed that in some mutants carpals, metacarpals, or even stunted phalanges were formed, precise identification of these structures has yet to be carried out.

To determine the extent to which forelimb skeletal development was impacted by U11-loss, the long bones of mutant and wild-type littermates were compared based on three factors: shaft length, diaphysis width, and the extent to which the diaphysis had begun to ossify (**figure 7F**). When this analysis was conducted for the humerus, it was found that U11 loss resulted in a drastic decrease in length of approximately 74% (**figure 7**). A decrease in diaphysis width was also observed in mutant pups which possessed widths 0.21mm compared to 0.46mm of wild-type littermates (**figure 9**). To determine if the ossification of the humerus had been impacted in mutants due to U11 loss, the extent to which ossification had occurred was calculated as a percentage of the overall bone length. It was found that in wild-type humeri, approximately 66% of the total bone had begun to ossify by P0. However, in mutants there was a drastic decrease of alizarin red

staining which found that only 33.5% of the cartilage in mutant humeri had begun to ossify by P0 indicating either disruption or delay of bone formation in these mutants.

Similar analyses were competed for the distal long bones (radius/ulna). However, due to the extreme variability of developmental defects in the mutant forelimbs, analysis of these structures was limited. Mutants only possessed at most a single distal long bone. As such, this structure was compared to both the radius and ulna of wild-type littermates. The results of these analyses are summarized in **figure 9**. Despite the variability of this structure, the decrease in both length and width of the mutant distal long bone was significant when compared to either wild-type radii or ulnae. When compared to wild-type littermates, the mutant distal long bone showed a decrease in length of approximately 80% when compared to the ulna or 75% when compared to the radius (**figure 7**). As with the humerus, analyses of both diaphysis width and ossification were conducted comparing the mutant distal long bone to both wild-type ulnae and radii. It was found that the width of the mutant long bone decreased by 60% when compared to wild-type ulnae, and 50% for the radii. Meanwhile ossification was reduced by approximately 75% when compared to both wild-type long bones (**figure 9**).

The disruption to the hindlimb of mutants is not as drastic as that of the forelimb, and all skeletal components found in wild-type hindlimbs are present in mutants (**figure 8A**). In fact, several bone markings which can be observed on wild-type long bones can be found in the mutants as well. In wild-type femora, bone markings which can be discerned include the greater trochanter, the third trochanter, and the lateral and medial condyles (**figure 8B**). All four of these can also be found in the mutant limbs, making this the only mutant long bone with identifiable bone markings (**figure 8D**).

As with the forelimb, the extent to which loss of U11 has impacted hindlimb bone growth was determined based on analyses of bone length, width, and ossification percentage. While changes were not as extreme as in the humerus, mutant femurs were significantly shorter than those of wild-type litter mates. The overall length of these bones had decreased from approximately 3.9mm in wild-type pups to 1.9mm in mutants (**figure 8**). In addition, the diaphysis width had also been reduced by approximately 44% and the extent of ossification had decreased by 14% (**figure 8)**.

In wild-type mice both the tibia and fibula expected to be relatively close in length to the femur by P0: approximately 4.1mm and 3.8mm respectively. In mutants it was found that both of these bones significantly decreased in length with mutant tibiae reaching approximately 1.4mm and 1.4 for the fibula. A significant decrease in diameter of the diaphysis of these bones also occurred in mutant mice with the tibia going from 0.48mm in wild-type mice to no more than 0.22mm in mutants (**figure 9**). A similar decrease in width occurs in the mutant fibulae which are approximately 0.17mm in width compared to 0.24mm in wild-type littermates (**figure 9**). Ossification in both distal long bones of the hind limb appears to be either disrupted or delayed by P0 as the extent to which calcified tissue could be stained by alizarin red decreased from 63.8% in wild-type pups to 44.5% for mutant tibia. The fibulae experienced a similar decrease in ossification; going from 64.1% in wild-type littermates to 43.5% in mutants (**figure 9**).

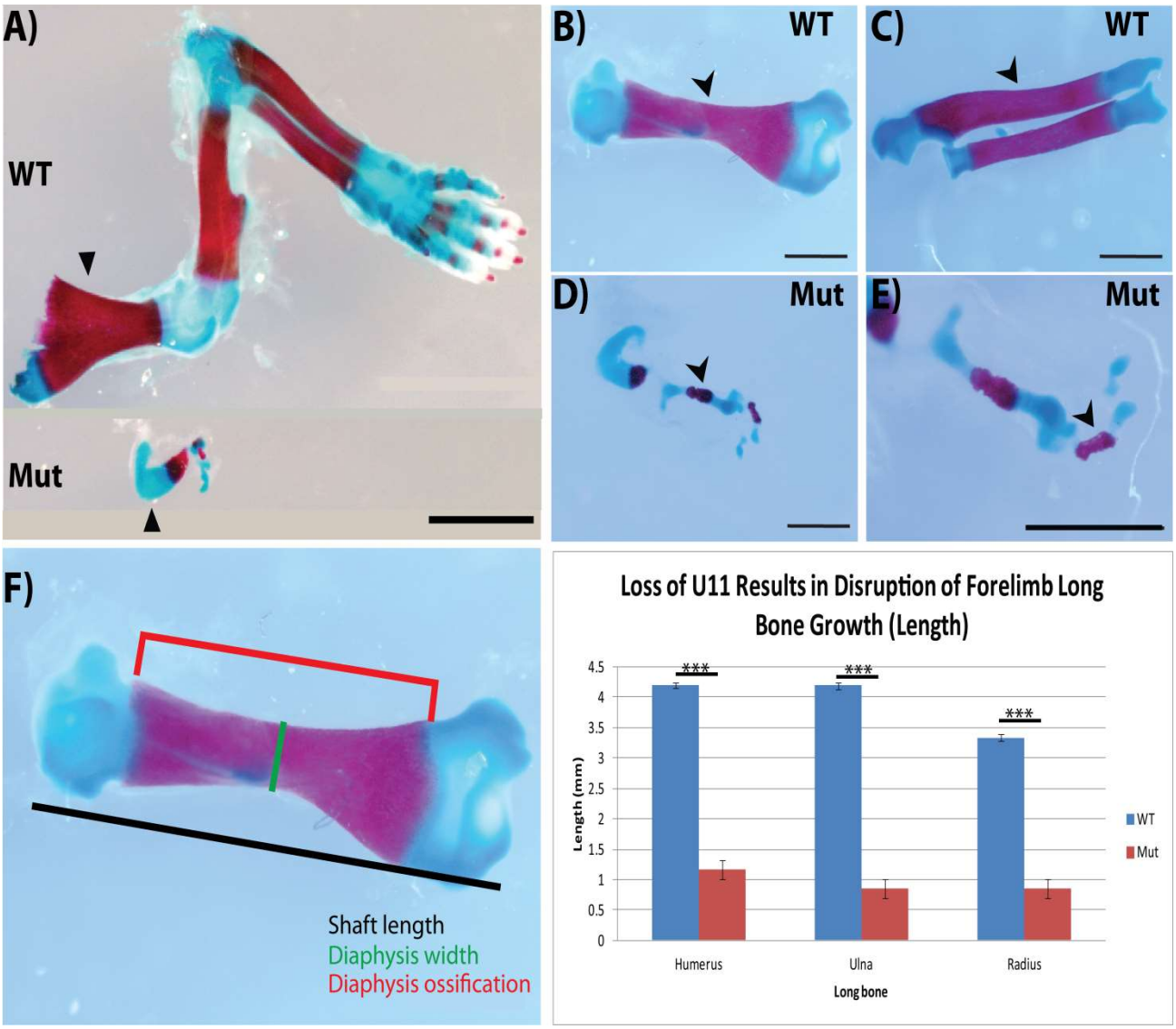

Figure 7. U11 loss results in defects of forelimb patterning and development by P0. A) Comparison of P0 forelimbs of wild-type and U11 cKO littermates. Ossifying boney elements are stained red while unossified cartilage is stained blue. Arrows mark the developing scapula of both limbs. **B/D)** The humerus of wild-type mice is significantly larger than that of U11 cKO mice. Arrows mark the ossifying diaphysis of these developing long bones. **C/E)** Unlike wild-type pups which poses two distal long bones, only a single long bone forms in the U11 cKO zeugopod region. Due to its articulation with the humerus, it is believed that this long bone is likely a ulna. **F)** Long bone growth was calculated based on three aspects i) total bone length measured from epiphysis to epiphysis end, ii) Diaphysis width at the center of long bone ossification, and iii) percent of long bone ossification calculated as length of ossified region/total bone length. As only a single distal long bone was present in mutant pups, this bone was compared to both the ulna and radius of wild-type littermates. Comparisons of forelimb long bone length are displayed in graph form. **n=3, *p<.05, **p<.005, ***p<.005. Scale bars: A (2.0mm) B-E (1.0mm)**

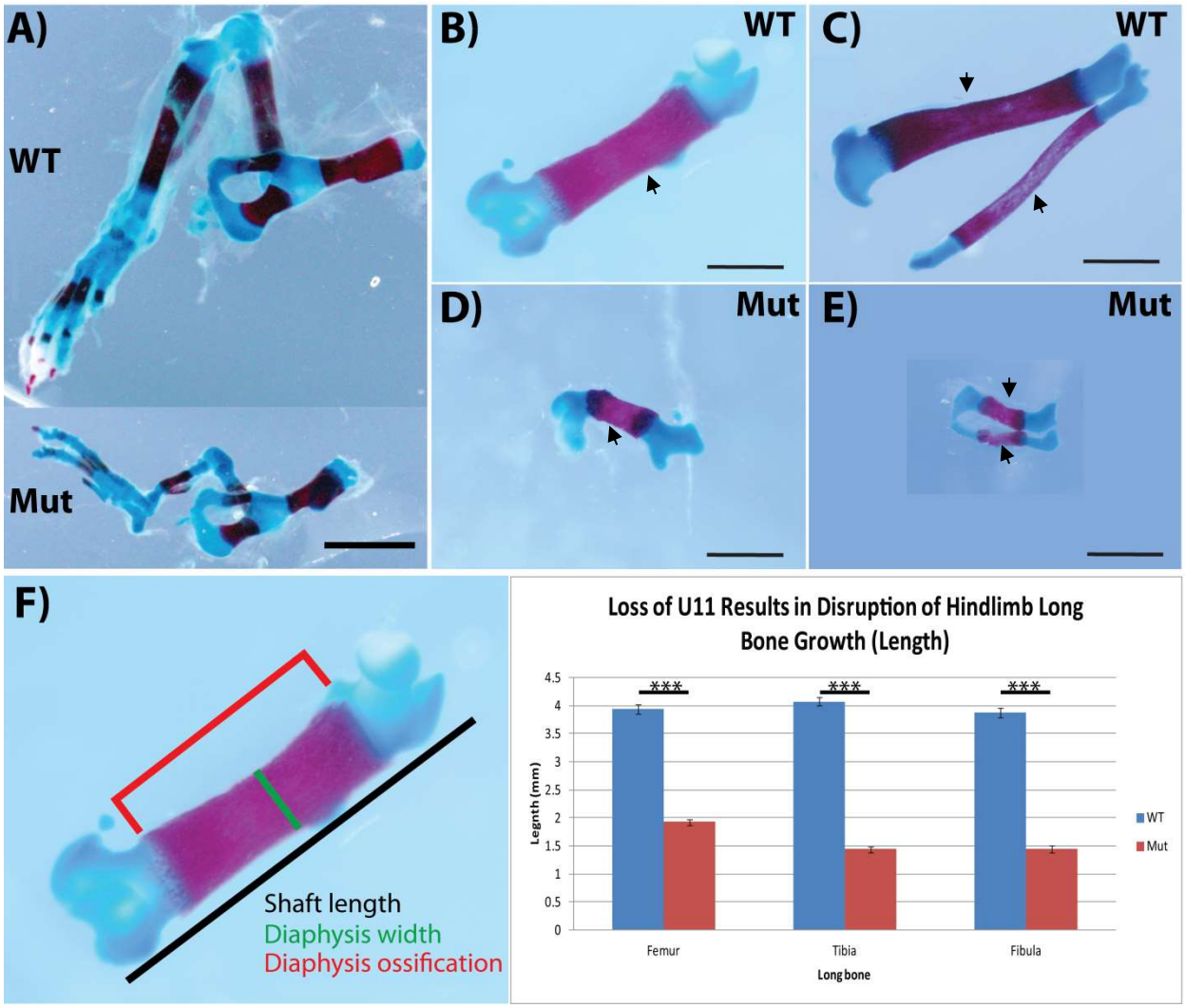

Figure 8: Loss of U11 results in defects of hindlimb development by P0. A) Comparison of P0 hindlimbs of wild-type and U11 cKO littermates. Ossifying boney elements are stained red while unossified cartilage is stained blue. **B/D)** The femur of wild-type mice is significantly larger than that of U11 cKO mice. Arrows mark the ossifying diaphysis of these developing long bones. **C/E)** Unlike in the forelimb, both wild-type and U11 cKO mutants poses two distal long bones. **F)** As with the forelimb, long bone growth was calculated based on three aspects i) total bone length measured from epiphysis to epiphysis end, ii) Diaphysis width at the center of long bone ossification, and iii) percent of long bone ossification calculated as length of ossified region/total bone length. As only a single distal long bone was present in mutant pups, this bone was compared to both the ulna and radius of wild-type littermates. Comparisons of forelimb long bone length are displayed in graph form. **n=6, *p<.05, **p<.005, ***p<.005. Scale bars: A (2.0mm) B-E (1.0mm)**

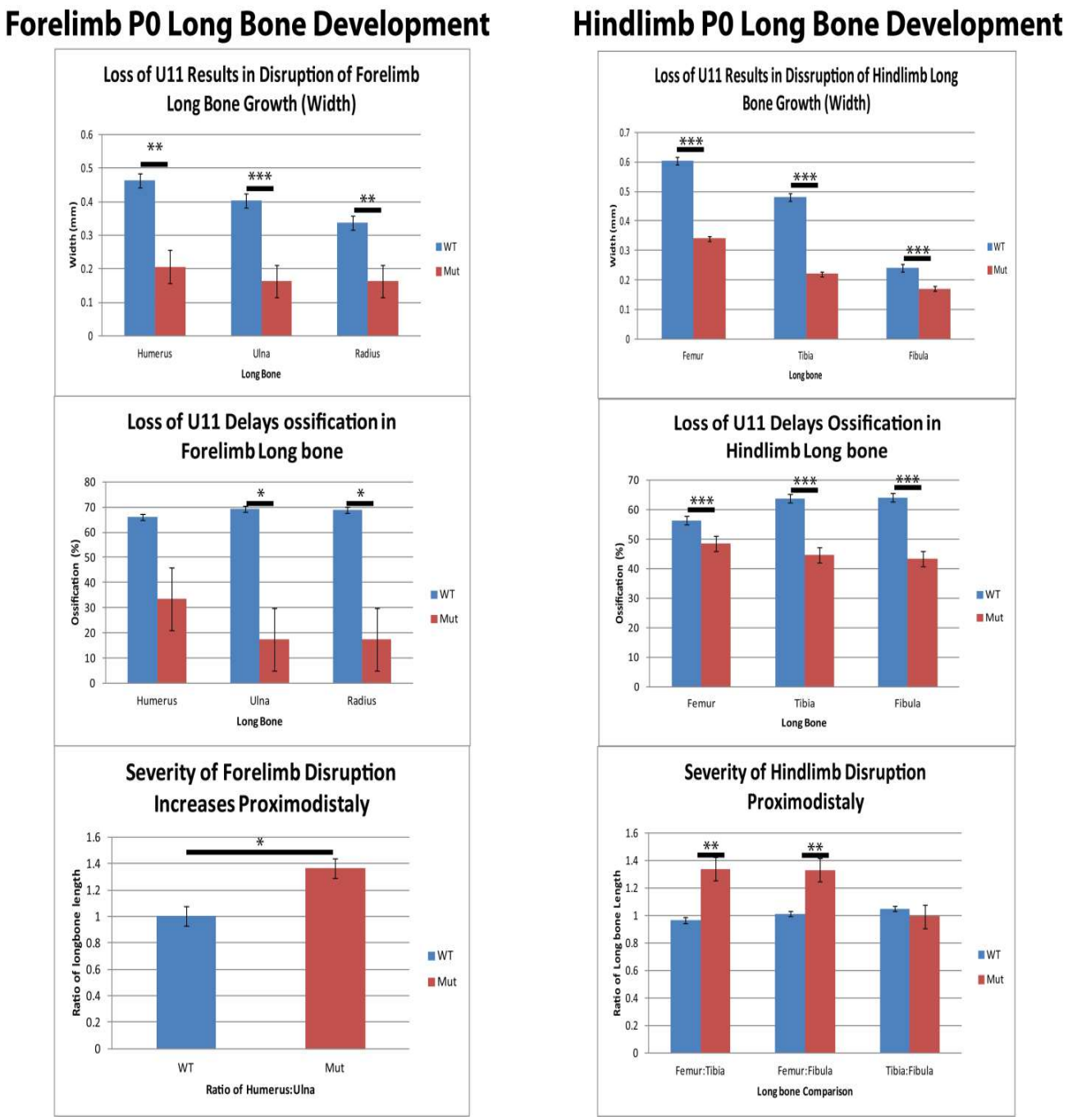

Figure 9: Summary of Skeletal Comparisons of P0 Limb Development Skeletal Comparison of P0 Hindlimbs. Long bone growth was determined based on 1) Total bone length measured from epiphysis to epiphysis end, 2) Diaphysis width at the center of long bone ossification, and 3) percent of long bone ossification calculated as length of ossified region/total bone length. In the hindlimb, shift in growth defect along the proximodistal axis was determined based on a ratio of proximal long bone length to that of the distal long bones. **Forelimb: n=3. Hindlimb: n=6. *p<.05, **p<.005, ***p<.005**

Loss of U11 Results in Disruption of Proliferating cells through death and disruption of cell cycle

While skeletal preparations reveal severe limb defects occur in U11 cKO mice by P0, better understanding of how this phenotype occurs requires investigation of limb growth during embryonic development. Such disruption could be the result of several factors, including depletion of the progenitor cell pool early in development or loss of patterning within the limb. In order to begin understanding which could be the case, I first investigated the kinetics of U11 expression in wild-type limb buds, as well as U11 loss in mutant limbs.

In situ hybridization (ISH) was conducted using a U11 RNA probe. By E11 there appears to be a decrease in U11 expression in mutants when compared to wild-type littermates in the forelimb (**figure 10A**). This loss of U11 increases over time and by E12 there appears to be total absence of U11 in the majority of the developing forelimb mesenchyme. U11 is still present in the overlying ectoderm, which is unaffected by the Prrx1-cre. At E14, initial patterning of the forelimb is finished in the wild-type mice and long bones of the forelimbs can be viewed. In wild-type mice, U11 is expressed both in the connective tissue and in the chondrocyte condensations. However, in the mutant, we observed a lack of U11 expression in the chondrocyte population of the forelimb, whereas the connective tissue was U11-positive in some regions. These U11-null condensations are fated to form the skeletal components of the forelimb and were identified by expression of Sox9 (Data not shown) (**figure 10A**). The presence of U11 within surrounding connective tissue is likely the result of a delay in prrx1 activity.

In the E11 hindlimb there is little discernable change in U11 expression between mutant and wild-type mice, likely due to the delayed onset of Prrx1-cre in this region (**figure 10B**). However, by E12 there is a noticeable decrease in U11 expression in the hindlimb mesenchyme of mutant mice (**figure 10B**). At E14, the hindlimb of wild-type mice has been completely patterned and U11 expression can be seen in the surrounding connective tissue of the limb, as well as within the chondrocytes of the long bone itself. Unlike in the forelimb, by E14 the hindlimb of mutants appears to be patterned similarly to wild-type mice. However, while U11 can be seen in surrounding connective tissue of these mutants, the developing long bones lack any U11 expression. This is not the case for wild-type long bones which are clearly expressing U11 at this time (**figure 10B**). In summation, U11 is expressed throughout the limb bud mesenchyme of both the fore- and hindlimb of wild-type mice at E11. This expression continues through E12, up to E14 where U11 is expressed in both the chondrocytes of the developing long bone, as well as surrounding connective tissue. In mutant mice is a noticeable decrease of U11 expression in the E11 forelimb, however, hindlimb loss of U11 does not occur until E12. By E14 the forelimb has completely lost structural integrity, and U11 is absent in the chondrocyte populations which would normally contribute to the developing long bones. In the E14 mutant hindlimb long bones have developed, though there is a clear loss of U11 expression in the chondrocyte populations of this region.

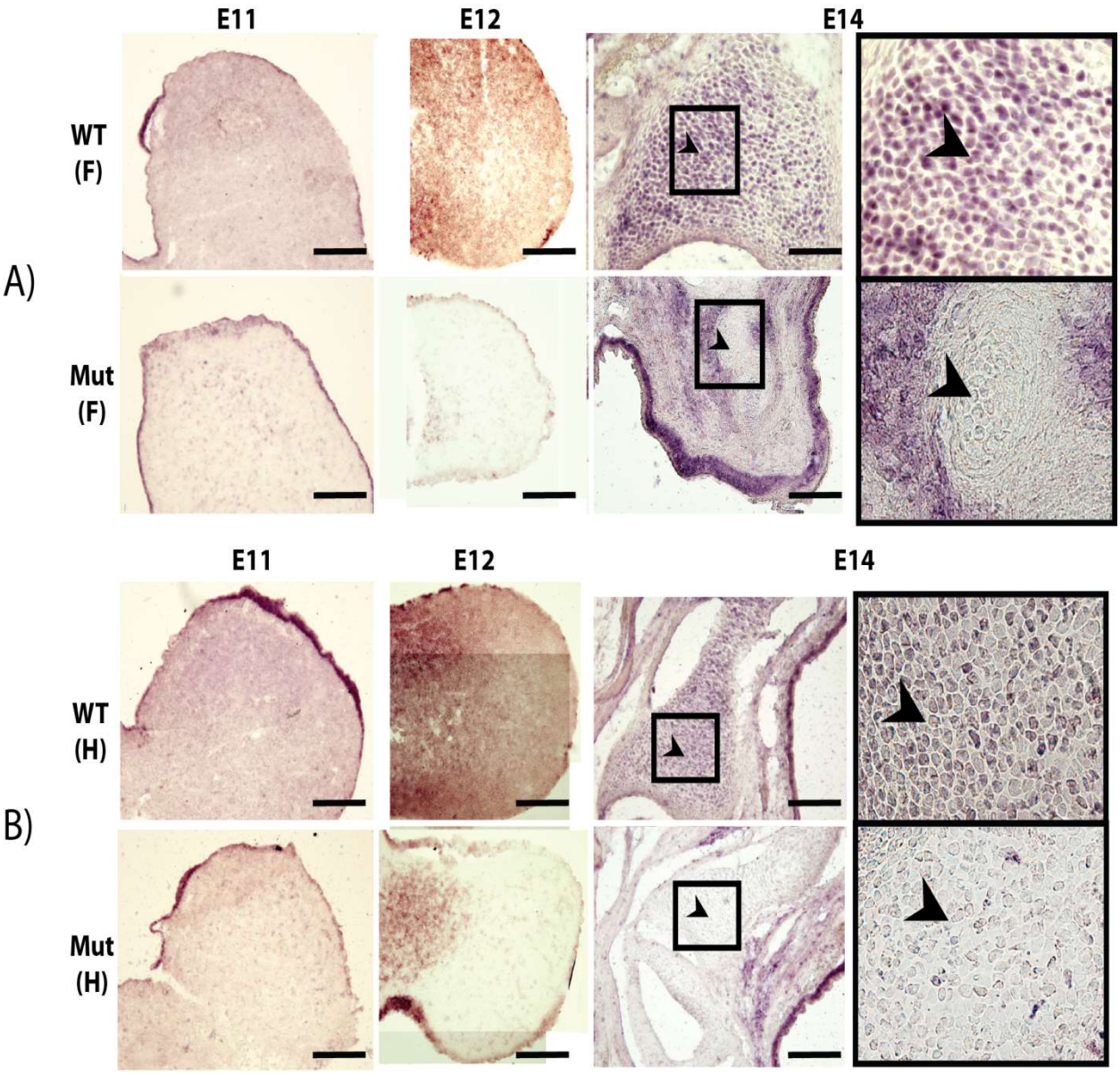

Figure 10: Kinetics of U11 loss in the limb-specific cKO. A) Alkaline phosphatase section in situ staining with U11 riboprobe shows that by E11 there is already a decrease in U11 expression within the forelimb (F) of cKO mutants. By E12 U11 has been lost entirely from the forelimb mesenchyme of mutants, but is still visible in wild-type littermates. At E14 chondrocytes (marked with arrows) which have been identified using Sox9 (data not shown) are still expressing U11 in wild-type forelimbs. However these same cells are completely null for U11 in mutant forelimbs. B) Similar analyses in the hindlimb (H) show that U11 is still present in the limb mesenchyme through E11 before dropping drastically by E12. Unlike in the forelimb, bones have patterned in the mutant hindlimb. However, the chondrocytes in these regions are null for U11, unlike wild-type bones which clearly demonstrate U11 expression.

To determine if the limb phenotypes observed in P0 mutants were the result of a decrease in the early progenitor cell pool, immunohistochemistry was performed on cryosections of wild-type and mutant limbs from E11, E12, and E14. To investigate whether U11 loss could result death of these progenitors, terminal deoxynucleotidyl transferase dUTP nick end labeling (TUNEL) assays were used to visualize any change in the rate of apoptosis between wild-type and mutant limbs. Ki67 and PH3 were utilized as markers of cell cycle to investigate if any shifts occurred in proliferating cell populations. Severe disruption of the mutant forelimb made equivalent comparisons with wild-type sections inaccurate; therefore analyses were carried out using the less compromised hindlimb as a model.

When E11 hindlimbs were analyzed, no significant difference was found between the percentage of TUNEL-positive cells in wild-type or mutant tissue (**figure 11A**). To determine if progenitor cells of the developing hindlimb were impacted by U11 loss, Ki67 was used to identify all cells in the cell cycle, and phosphohistone H3 was used as a M-phase specific marker. In E11 wild-type hindlimb buds, almost the entirety (99.7%) of the total mesenchyme cell population was Ki67-positive (**figure 12A**). The number of these cells which are also PH3 positive is much lower (5.6%), indicating that most of the proliferating limb mesenchyme exists outside of M-phase (**figure 12A**). In the mutant hindlimb there appears to be no significant difference between either Ki67 or PH3 expressing cells when compared to wild-type embryos, indicating that at E11 there is no observable change to the progenitor cell pool in U11 cKO mutants.

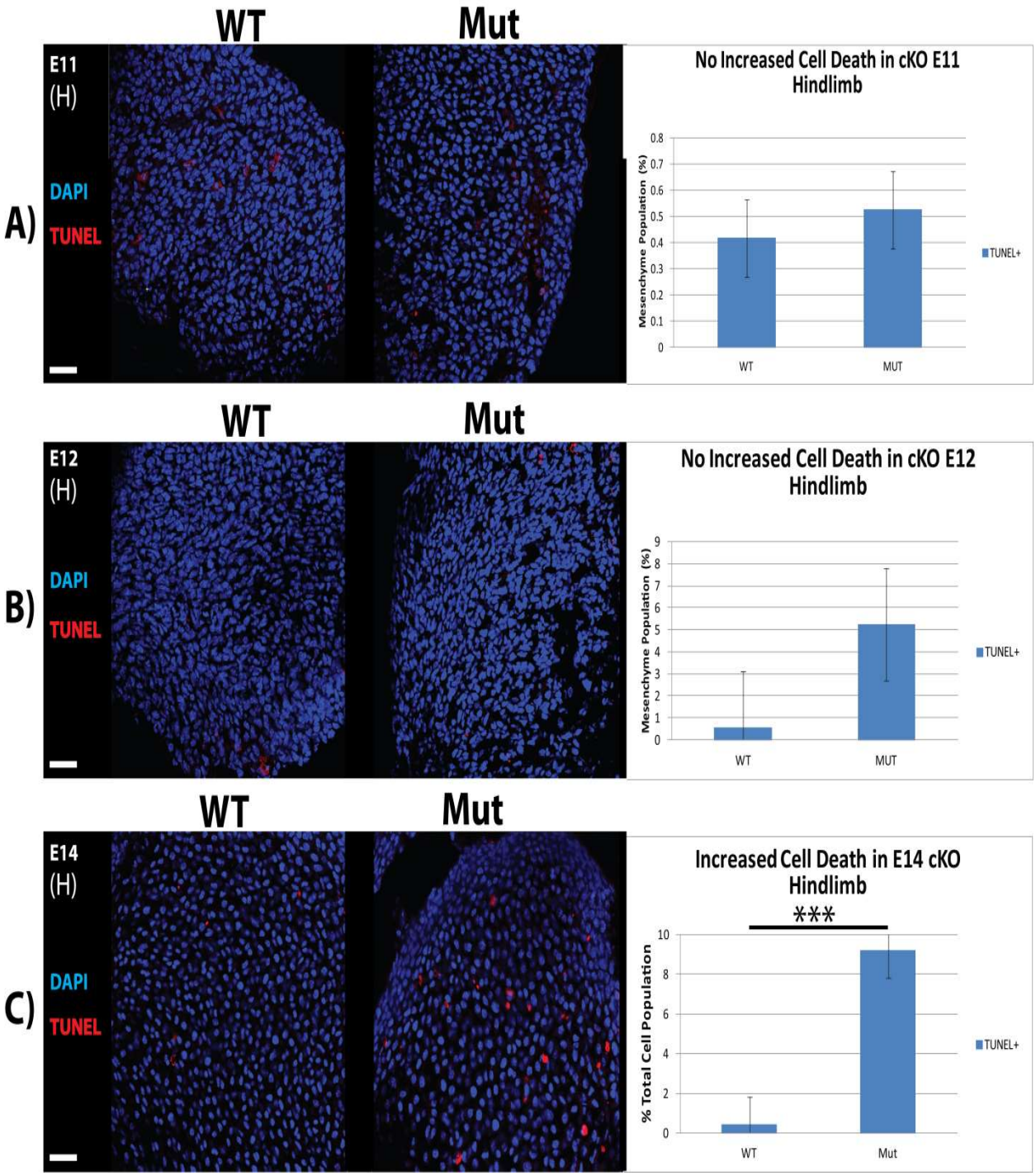

Figure 11. TUNEL assay of U11 cKO shows increased cell death by E14. A) At E11 identification of TUNEL-positive cells shows no significant increase of cell death in the hindlimb (H) of U11 cKO mice. TUNEL+ percentages were calculated as number of TUNEL positive cells over the number of total DAPI stained nuclei per field. **B)** By E12 a slight increase in cell death can be detected, however it has not been shown to be statistically significant. **C)** In E14 mutant hindlimbs there is a drastic increase in apoptotic cells when compared to wild-type littermates. **Scale bar= 30um. E11 n=3, E12 n=3, E14 n=3. *p<.05, **p<.005, ***p<.005.**

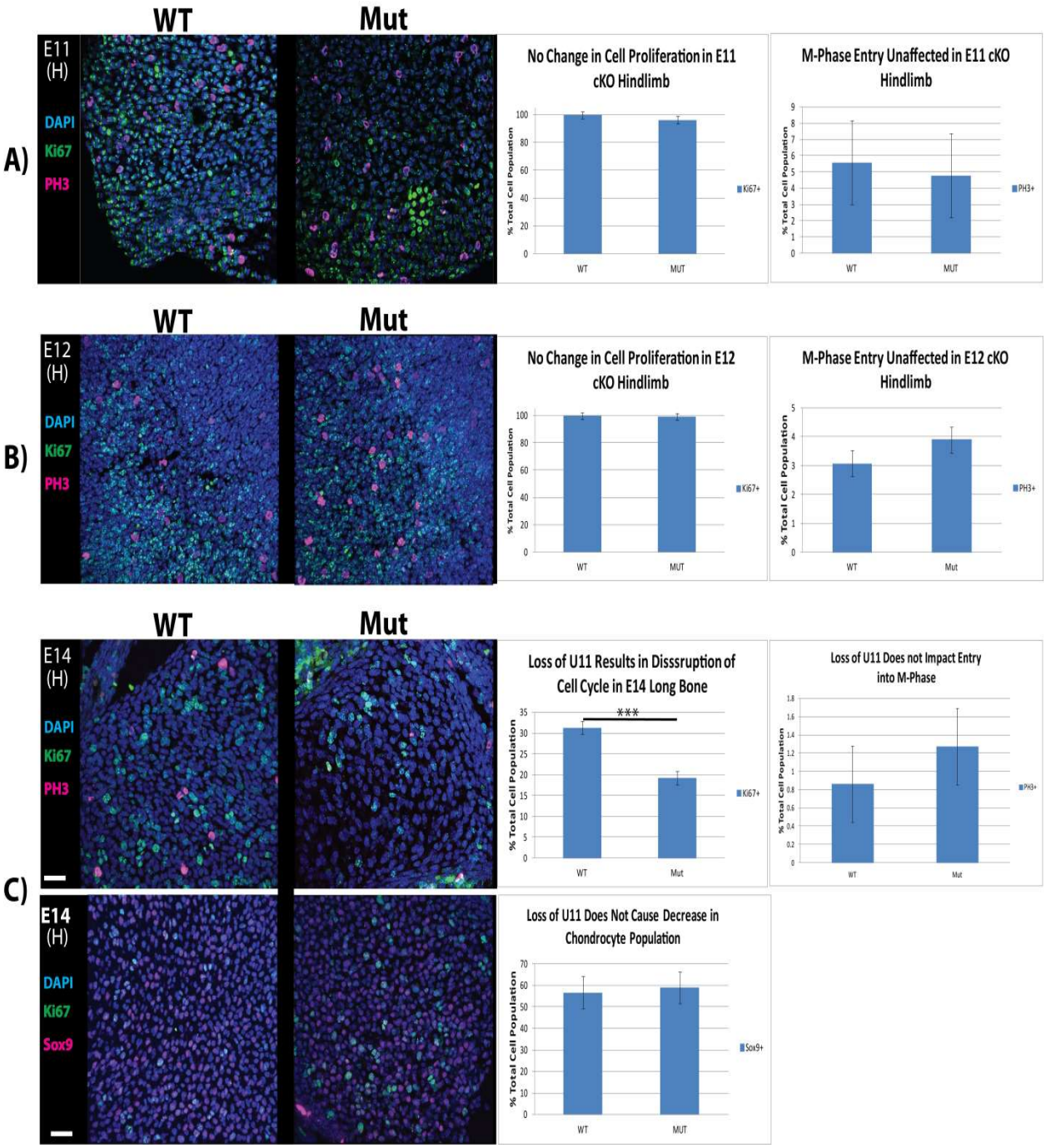

Figure 12: U11cKO show decrease in proliferating cells through Ki67 Staining by E14 A) At E11 immunofluorescent identification of proliferating cells through a combination of Ki67 and PH3 markers shows no significant change between wild-type and U11 cKO hindlimb (H). **B)** At E12 a decrease in Ki67-positive cells can be observed, however at this time the change is not statistically significant. **C)** By E14 there is a significant decrease in proliferating cells within the mutant hindlimb. Sox9 identification of differentiating chondrocytes shows no difference in chondrocyte populations between wild-type and mutant hindlimbs. **Scale bar= 30um. E11 n=2, E12 n=3, E14 n=3. *p<.05, **p<.005, ***p<.005**

TUNEL assays conducted at E12 found that while there was an increase in the number of TUNEL-positive cells in the mutant hindlimb, this difference was not statistically significant (**figure 11B**). Similarly, when analyses were conducted for Ki67 at this time point it was found that while there was a slight decrease in Ki67-positive cells from 99.5% in wild-type hindlimbs to 99.1% in mutants, this change was not statistically significant. As with Ki67, comparison of PH3-positive cells in the mutant hindlimb with that of wild-type littermates demonstrated no statistically significant change. (**figure 12B**).

Unlike at earlier time points, the developing bones of E14 mutants showed an extensive increase in TUNEL-positivity. In wild-type mice, less than <1% of cells within the developing long bone were stained by TUNEL assay. However, in mutants this increased to almost 10% (**figure 11C**). The number of Ki67-positive cells within the developing bones also showed a significant change from wild-type values, decreasing from 32.0% to approximately 20.7% (**figure 12C**). At this time there is no significant increase in PH3 expression.

By this time in development, the hindlimb of wild-type mice is fully patterned, and the cartilaginous condensations which form the scaffolding of future bones consist of a mixture of proliferating progenitor cells, as well as differentiated chondrocytes. To determine if differentiation of chondrocytes had been impacted in mutant hindlimbs, Sox9 was used to analyze the chondrocyte population in the epiphyseal regions of the hind limbs. It was found that in wild-type hindlimbs approximately 56% of the developing bone was Sox9-positive. In mutants this population composed 58% of cells within the bone indicating no significant shift in chondrocyte populations within the developing limb (**Figure 12C**).

Discussion

While minor splicing is required for the processing of a relatively small number of introns (<0.5%), its importance is highlighted by the conservation of this secondary set of splicing machinery across eukaryotic evolution.[15,16] However, while knockout studies in a wide-range of species have demonstrated the necessity of minor splicing in early eukaryotic development, it is still unknown what essential role this second spliceosome plays which has allowed it to persist. The identification of *Rnu4atac* mutations in MOPDI and Roifman syndrome patients allows for a correlation to be drawn between minor splicing and the pathology of these diseases. However, these studies have remained descriptive in humans, and while it has been shown that MOPDI associated mutations can decrease efficacy of minor splicing, a causative effect of minor splicing in the pathogenesis of these diseases has not been found.[1,2]

To elucidate what role minor splicing may play in limb development we employed a limb specific conditional KO of U11. By targeting minor splicing in the developing limb bud through a non-U4atac dependent manner we were able to induce limb disruption that, while far more severe than that observed in MOPDI patients, confirms the requirement of minor splicing in limb development. The extent to which cKO of U11 causes loss of limb development in mice is drastic, and even between the forelimb and hindlimb there is variability in the degree of this disruption. While possibly indicating region specificity of minor splicing requirement, more likely this difference is a result of variability in prrx1-cre activation between the two limb systems.

Within the forelimb, prrx1-cre recombination occurs as early as E9 and is pervasive throughout the entirety of the limb bud mesenchyme. However in the hindlimb cre-activity

is delayed, and even by E10.5 there are regions within the mesenchyme that still do not express cre.[65] It is interesting that this temporal variability could result in such a drastic change in phenotype, and offers a comparison of how the impact of minor splicing loss within the limb can be time dependent.

Analysis of the skeletal components of P0 U11 cKO mice reveal that even in the forelimb, though structural integrity has been almost entirely lost, skeletal elements of all three limb regions (stylopod, zeugopod, and autopod) are present to varying degrees (figure 11A). Though the development of these regions has been compromised by U11 cKO, their presence indicates that early patterning if the proximodistal axis has been successfully laid down in the forelimb. This is confirmed in the hindlimb phenotype where, though growth has been reduced in the cKO mutants, all skeletal elements are present.

As it appears that initial patterning is not lost due to disruption of minor splicing, a possible path through which U11 cKO could disturb skeletal development in the limbs is through reduction of early progenitor cell populations. It is established that proliferation of limb progenitors is required for limb development. FGFR2 knockout experiments conducted by Lu et al. have demonstrated that if the AER is not maintained in developing mouse limbs, it can result in a reduced progenitor population within the limb bud. This pool, if insufficient, will fail to establish the rudimentary skeletal populations necessary to generate autopod condensations, resulting in loss of distal limb structures.[66] This type of proximal to distal bias is reflected in both the forelimb and hindlimbs of U11 ckO mutants (figure 9). Could U11 loss then be disrupting early progenitor cells? Indeed, work investigating loss of U11 in the developing brain has already demonstrated that U11 might

be necessary for maintenance of CNS progenitor cells.[25] We therefore investigated how loss of minor splicing could affect progenitor cells in the limb.

One such impact which might occur would be a decrease in the population of limb progenitors through increased cell death. *In situ* analysis of the kinetics of U11 loss in the mutant hindlimb reveals that knockout of U11 from the limb bud mesenchyme does not occur until around E12 (**figure 10**). Therefore, it is unlikely that any significant change in the mutant progenitor survival would occur before that time. Indeed, no significant increase in TUNEL-positivity was detected in U11 cKO mouse hindlimbs prior to E12. However, by E14 the number of dying cells in the developing mutant bones does increase significantly between wild-type and mutants (**figure 11**). This would indicate that an increase in apoptosis could possibly contribute to the skeletal defects observed at P0. However, the percentage of dying cells within the developing bones, even at E14, is relatively small. Therefore it is unlikely that cell death alone constitutes a loss of progenitor cells impactful enough to result in the phenotype observed.

As cell death alone is likely not the sole driving force behind the disruption of mutant long bone growth, we next looked to how the proliferating progenitors of the limb were altered due to U11 loss. Using Ki67 and Ph3 to mark proliferating cells it was found that at E11 there is no difference between wild-type and mutant hindlimb mesenchyme proliferation. However, this begins to change as U11 is lost, and by E12 there is a slight (though not yet statistically significant) decrease in Ki67-positive cells in the mutants. At E14 this shift in progenitors out of cell cycle is even more pronounced, as there is a 42% decrease in the number of proliferating cells between wild-type and mutant embryos.

This loss of proliferating cells could be attributed to two possible factors. First it could result from an increased exit of progenitor cells from cell cycle. Alternatively, increased differentiation of progenitors to chondrocytes might be reflected in a shift away from proliferation. Marking of cells with Sox9 shows no significance change between wild-type and mutant mice in the percentages of differentiating chondrocytes. This in turn indicates that though loss of U11 does decrease the number of cells in cell cycle, it does not appear to shift the percentage of differentiating cells.

How then do these results explain the severe phenotype we see by P0? It is likely that loss of minor splicing specifically impacts the proliferating mesenchyme of the early limb bud, depleting this central pool of progenitors through a combination of cell-cycle exit and death. Initial patterning of the proximodistal axis of the mouse limb is unaffected by U11 loss, as evidenced by the proper patterning of all skeletal elements of the U11 cKO hindlimb as well as the presence of at least some distal structures in the mutant forelimb. The presence of such structures is indicative of successful early patterning of progenitor populations as suggested by the early differentiation front model of limb development.[53] Therefore, loss of proliferating progenitors appears the most likely cause of the developmental defects observed in U11 cKO limbs.

Conclusion and Future Directions

My results reveal that minor splicing is essential for limb development in mice, and that loss of this cellular process likely impacts proliferating progenitor cells early in development. It has been well established that minor splicing is essential for development in eukaryotes.[1-5] Yet while mutations resulting in MOPD and Roifman syndrome have led to a correlation between minor splicing and limb development, this is the first known instance of utilizing direct loss of a minor splicing component to investigate limb development in mice. Using this model we have demonstrated that loss of U11 causes a decrease in the number of proliferating cells within the developing mouse limb due to a combination of cell death and an exiting of cells from cell cycle. This reduction in proliferating progenitors in turn results in severe disruption of limb growth by P0.

While it is likely that U11 is necessary for maintenance of progenitors within the developing mouse limb, it also is possible that the phenotype observed in U11 cKO mice could be the result of a loss of limb patterning through indirect influence on the signaling centers within the limb. Several regions within the limb must communicate for limb growth and patterning to occur. The AER and ZPA in particular are essential in not only patterning the limb's proximal-distal and anterior-posterior axes, but also in the maintenance of one another through the SHH-GREM1-FGF feedback loop. Prrx1-cre is not expressed in the AER, therefore making it unlikely that U11 loss is impacting this region directly.[65] However, by disturbing the mesenchyme required for relaying SHH signaling through GREM1 activity, it might be possible that U11 loss is indirectly leading to disturbance of the feedback loop necessary for maintenance of the AER. Indeed, preliminary data has suggested that in U11cKO mutants, there might be an increased percentage of dying

cells within the presumptive AER, despite continued U11 expression (data not shown). To confirm whether U11 cKO mutants are experiencing patterning disruption though such a pathway, further work should be conducted focusing on both the impact of U11 loss on limb signaling centers, and at the underlying molecular shifts occurring due to U11 cKO.

One path of continuing investigation could be employment of whole-mount *In situ* hybridization to determine if there is a shift in the expression of essential signaling molecules including FGFs, SHH, BMPs, and GREM1 within the U11 cKO limbs. Additionally, further analysis of molecular changes within the mutant limbs could be examined through the use of RNA sequencing. Such an analysis has already been conducted in U11-null tissue of the developing mouse CNS.[25] This study demonstrated that cKO of U11 resulted in differentiating expression of MIGs linked to many different cellular processes. Among those impacted were systems required for cell cycle and cell survivability. If a similar shift in MIG expression is found in our limb-specific U11 cKO, this could credence to the role of minor splicing In maintaining proliferation of progenitors in the developing limb bud.

References

1. Majewski, F., M. Stoeckenius, H. Kemperdick, and John M. Opitz. "Studies of Microcephalic Primordial Dwarfism III: An Intrauterine Dwarf with Platyspondyly and Anomalies of Pelvis and Clavicles—osteodysplastic Primordial Dwarfism Type III." American Journal of Medical Genetics Am. J. Med. Genet. 12.1 (1982): 37-42.

2. He, H., S. Liyanarachchi, K. Akagi, R. Nagy, J. Li, R. C. Dietrich, W. Li, N. Sebastian, B. Wen, B. Xin, J. Singh, P. Yan, H. Alder, E. Haan, D. Wieczorek, B. Albrecht, E. Puffenberger, H. Wang, J. A. Westman, R. A. Padgett, D. E. Symer, and A. De La Chapelle. "Mutations in U4atac SnRNA, a Component of the Minor Spliceosome, in the Developmental Disorder MOPD I." *Science* 332.6026 (2011): 238-40.

3. Merico, Daniele, Maian Roifman, Ulrich Braunschweig, Ryan K. C. Yuen, Roumiana Alexandrova, Andrea Bates, Brenda Reid, Thomas Nalpathamkalam, Zhuozhi Wang, Bhooma Thiruvahindrapuram, Paul Gray, Alyson Kakakios, Jane Peake, Stephanie Hogarth, David Manson, Raymond Buncic, Sergio L. Pereira, Jo-Anne Herbrick, Benjamin J. Blencowe, Chaim M. Roifman, and Stephen W. Scherer. "Compound Heterozygous Mutations in the Noncoding RNU4ATAC Cause Roifman Syndrome by Disrupting Minor Intron Splicing." Nature Communications Nat Comms 6 (2015): 8718.

4. Kim, Won Yong, Hyun Ju Jung, Kyung Jin Kwak, Min Kyung Kim, Seung Han Oh, Yeon Soo Han, and Hunseung Kang. "The Arabidopsis U12-Type Spliceosomal Protein U11/U12-31K Is Involved in U12 Intron Splicing via RNA Chaperone Activity and Affects Plant Development." The Plant Cell Plant Cell 22.12 (2010): 3951-962.

5. Markmiller, S., N. Cloonan, R. M. Lardelli, K. Doggett, M.-C. Keightley, Y. Boglev, A. J. Trotter, A. Y. Ng, S. J. Wilkins, H. Verkade, E. A. Ober, H. A. Field, S. M. Grimmond, G. J. Lieschke, D. Y. R. Stainier, and J. K. Heath. "Minor Class Splicing Shapes the Zebrafish Transcriptome during Development." Proceedings of the National Academy of Sciences 111.8 (2014): 3062-067.

6. Patel, Abhijit A., Matthew McCarthy, and Joan A. Steitz. “The Splicing of U12-Type Introns Can Be a Rate-Limiting Step in Gene Expression.” *The EMBO Journal* 21.14 (2002): 3804–3815. *PMC*. 1 July 2016.

7. Green, Michael R. "Biochemical mechanisms of constitutive and regulated pre-mRNA splicing." Annual review of cell biology 7.1 (1991): 559-599.

8. Burge, Christopher B., Thomas Tuschl, and Phillip A. Sharp. "20 Splicing of Precursors to mRNAs by the Spliceosomes." Cold Spring Harbor Monograph Archive 37 (1999): 525-560.

9. Black, Douglas L. "Mechanisms of alternative pre-messenger RNA splicing." Annual review of biochemistry 72.1 (2003): 291-336.

10. Burge, Christopher B., Richard A. Padgett, and Phillip A. Sharp. "Evolutionary Fates and Origins of U12-Type Introns." Molecular Cell 2.6 (1998): 773-85.

11. Senapathy, Periannan, Marvin B. Shapiro, and Nomi L. Harris. "[16] Splice Junctions, Branch Point Sites, and Exons: Sequence Statistics, Identification, and Applications to Genome Project." Methods in Enzymology (1990): 252-78.

12. Sharp, Phillip A., and Christopher B. Burge. "Classification of Introns: U2-Type or U12-Type." Cell 91.7 (1997): 875-79.

13. Gao, K., A. Masuda, T. Matsuura, and K. Ohno. "Human Branch Point Consensus Sequence Is YUnAy." Nucleic Acids Research 36.7 (2008): 2257-267.

14. Hall, Stephen L., and Richard A. Padgett. "Conserved Sequences in a Class of Rare Eukaryotic Nuclear Introns with Non-consensus Splice Sites." Journal of Molecular Biology 239.3 (1994): 357-65.

15. Basu, Malay Kumar, Wojciech Makalowski, Igor B. Rogozin, and Eugene V. Koonin. "U12 Intron Positions Are More Strongly Conserved between Animals and Plants than U2 Intron Positions." Biology Direct Biol Direct 3.1 (2008): 19.

16. Russell, Anthony G., J. Michael Charette, David F. Spencer, and Michael W. Gray. "An Early Evolutionary Origin for the Minor Spliceosome." Nature 443.7113 (2006): 863-66.

17. Jung HJ, Kang H. The Arabidopsis U11/U12-65K is an indispensible component of minor spliceosome and plays a crucial role in U12 intron splicing and plant development. Plant J. 2014 Jun;78(5):799-810.

18. Otake LR, Scamborova P, Hashimoto C, Steitz JA. The divergent U12-type spliceosome is required for pre-mRNA splicing and is essential for development in Drosophila. Mol Cell. 2002 Feb;9(2):439-46.

19. Taybi, Hooshang, and David Linder. "Congenital Familial Dwarfism with Cephaloskeletal Dysplasia 1." Radiology 89.2 (1967): 275-81.

20. Pierce MJ, Morse RP. The neurologic findings in Taybi-Linder syndrome (MOPD I/III): case report and review of the literature. Am J Med Genet A. 2012 Mar;158A(3):606-10.

21. Roifman, C. M. Immunological aspects of a novel immunodeficiency syndrome that includes antibody deficiency with normal immunoglobulins, spondyloepiphyseal dysplasia, growth and developmental delay, and retinal dystrophy. Canad. J. Allergy Clin. Immun. 2: 94-98, 1997

22. Roifman, C. M. Antibody deficiency, growth retardation, spondyloepiphyseal dysplasia and retinal dystrophy: a novel syndrome. Clin. Genet. 55: 103-109, 1999.

23. Fairchild, H. R., Fairchild, G., Tierney, K. M., McCartney, D. L., Cross, J. J., de Vries, P. J. Partial agenesis of the corpus callosum, hippocampal atrophy, and stable intellectual disability associated with Roifman syndrome. Am. J. Med. Genet. 155A: 2560-2565, 2011.

24. Gray, P. E. A., Sillence, D., Kakakios, A. Is Roifman syndrome an X-linked ciliopathy with humoral immunodeficiency? Evidence from 2 new cases. Int. J. Immunogenet. 38: 501-505, 2011.

25. Baumgartner M, Olthof A. Lemoine C, Seesi,S, Hyatt K, Sturrock N, Nguyen N, Goz R, LoTurco J, Kanadia R. MOPD1-like microcephaly caused by inactivation of the minor spliceosome in the developing mouse cortex. **In review**, 2016.

26. Wanek, N., K. Muneoka, G. Holler-Dinsmore, R. Burton, and S. V. Bryant. "A Staging System for Mouse Limb Development." J. Exp. Zool. Journal of Experimental Zoology 249.1 (1989): 41-49.

27. Milaire, J., and J. Mulnard. "Histogenesis in 11-day Mouse Embryo Limb Buds Explanted in Organ Culture." J. Exp. Zool. Journal of Experimental Zoology 232.2 (1984): 359-77.

28. Tickle, C., B. Alberts, L. Wolpert, and J. Lee. "Local Application of Retinoic Acid to the Limb Bond Mimics the Action of the Polarizing Region." Nature 296.5857 (1982): 564-66.

29. Stratford, Thomas, Claire Horton, and Malcolm Maden. "Retinoic Acid Is Required for the Initiation of Outgrowth in the Chick Limb Bud." Current Biology 6.9 (1996): 1124-133.

30. Niederreither, K., Subbarayan, V., Dolle, P. & Chambon, P. 1999. Embryonic retinoic acid synthesis is essential for early mouse post-implantation development. Nat. Genet. 21, 444–448.

31. Mic, F. A., Haselbeck, R. J., Cuenca, A. E. & Duester, G. 2002. Novel retinoic acid generating activities in the neural tube and heart identified by conditional rescue of Raldh2 null mutant mice. Development 129, 2271–2282.

32. Zhao, X., Sirbu, I. O., Mic, F. A., Molotkova, N., Molotkov, A., Kumar, S. & Duester, G. 2009. Retinoic acid promotes limb induction through effects on body axis extension but is unnecessary for limb patterning. Curr. Biol. 19, 1050–1057.

33. Ohuchi H, 11 others The mesenchymal factor, FGF10, initiates and maintains the outgrowth of the chick limb bud through interaction with FGF8, and apical ectodermal factor. Development. 1997;124:2235–2244.

34. Sekine K, 10 others Fgf10 is essential for limb and lung formation. Nature Genet. 1999;21:138–141

35. Kawakami, Yasuhiko, Javier Capdevila, Dirk Büscher, Tohru Itoh, Concepción Rodríguez Esteban, and Juan Carlos Izpisúa Belmonte. "WNT Signals Control FGF-Dependent Limb Initiation and AER Induction in the Chick Embryo." Cell 104.6 (2001): 891-900.

36. M. Kengaku, J. Capdevila, C. Rodriguez-Esteban, J. De La Pena, R.L. Johnson, J.C.I. Belmonte, C.J. Tabin Distinct WNT pathways regulating AER formation and dorsoventral polarity in the chick limb bud Science, 280 (1998), pp. 1274–1277

37. Xu X L, 7 others Fibroblast growth factor receptor Z (FGFR2)-mediated reciprocal regulatory loop between FGF8 and FGF10 is essential for limb induction. Development. 1998;125:753–765

38. Yonei-Tamura S, Endo T, Yajima H, Ohuichi H, Ida H, Tamura K. FGF7 and FGF10 directly induce the apical ectodermal ridge in chick embryos. Dev. Biol. 1999;211:133–143.

39. Saunders, John W. "The Proximo-distal Sequence of Origin of the Parts of the Chick Wing and the Role of the Ectoderm." J. Exp. Zool. Journal of Experimental Zoology 108.3 (1948): 363-403.

40. Summerbell, D., J. H. Lewis, and L. Wolpert. "Positional Information in Chick Limb Morphogenesis." Nature 244.5417 (1973): 492-96.

41. Niswander, L., Tickle, C., Vogel, A., Booth, I. & Martin, G.R. FGF-4 replaces the apical ectodermal ridge and directs outgrowth and patterning of the limb. Cell 75, 579–587 (1993).

42. Fallon, J. et al. FGF-2: apical ectodermal ridge growth signal for chick limb development. Science 264, 104–107 (1994).

43. Crossley, P., Minowada, G., MacArthur, C. & Martin, G. Roles for FGF8 in the induction, initiation, and maintenance of chick limb development. Cell 84, 127–136 (1996).

44. Vogel, A., Rodriguez, C. & Izpisúa-Belmonte, J.-C. Involvement of FGF-8 in initiation, outgrowth and patterning of the vertebrate limb. Development 122, 1737–1750 (1996).

45. Crossley, P.H. & Martin, G.R. The mouse Fgf8 gene encodes a family of polypeptides and is expressed in regions that direct outgrowth and patterning in the developing embryo. Development 121, 439–451

46. Heikinheimo, M., Lawshé, A., Shackleford, G.M., Wilson, D.B. & MacArthur, C.A. Fgf-8 expression in the post-gastrulation mouse suggests roles in the development of the face, limbs, and central nervous system. Mech. Dev. 48, 129–138 (1994).

47. Mahmood, R. et al. A role for FGF-8 in the initiation and maintenance of vertebrate limb bud outgrowth. Curr. Biol. 5, 797–806 (1995).

48. Mariani, F. V., Ahn, C. P. & Martin, G. R. Genetic evidence that FGFs have an instructive role in limb proximal-distal patterning. Nature 453, 401–405 (2008).

49. Lewandoski, M., Sun, X. & Martin, G. R. Fgf8 signalling from the AER is essential for normal limb development. Nature Genet. 26, 460–463 (2000).

50. Dudley, A. T., Ros, M. A. & Tabin, C. J. A re-examination of proximodistal patterning during vertebrate limb development. Nature 418, 539–544 (2002).

51. Mercader, N. et al. Opposing RA and FGF signals control proximodistal vertebrate limb development through regulation of Meis genes. Development 127, 3961–3970 (2000).

52. Capdevila, J., Tsukui, T., Rodriquez Esteban, C., Zappavigna, V. & Izpisúa Belmonte, J. C. Control of vertebrate limb outgrowth by the proximal factor Meis2 and distal antagonism of BMPs by Gremlin. Mol. Cell 4, 839–849 (1999).

53. Tabin, C. & Wolpert, L. Rethinking the proximodistal axis of the vertebrate limb in the molecular era. Dev. 21, 1433–1442 (2007).

54. Chiang, C. et al. Manifestation of the limb prepattern: limb development in the absence of sonic hedgehog function. Dev. Biol. 236, 421–435 (2001).

55. Kraus, P., Fraidenraich, D. & Loomis, C. A. Some distal limb structures develop in mice lacking Sonic hedgehog signaling. Mech. Dev. 100, 45–58 (2001

56. Wolpert, L. Positional information and the spatial pattern of cellular differentiation. J. Theor. Biol. 25, 1–47 (1969).

57. Charite, J., McFadden, D. G. and Olson, E. N. (2000). The bHLH transcription factor dHand controls Sonic hedgehog expression and establishment of the zone of polarizing activity during limb development. Development 127,2461-2470

58. Marie Kmita, Basile Tarchini, Jozsef Zàkàny, Malcolm Logan, Clifford J. Tabin & Denis Duboule. Early developmental arrest of mammalian limbs lacking HoxA/HoxD gene function. Nature 435, 1113-1116 (2005)

59. Tarchini, B., Duboule, D. & Kmita, M. Regulatory constraints in the evolution of the tetrapod limb anterior–posterior polarity. Nature 443, 985–988 (2006).

60. Capellini, T. D. et al. Pbx1/Pbx2 requirement for distal limb patterning is mediated by the hierarchical control of Hox gene spatial distribution and Shh expression. Development 133, 2263–2273 (2006).

61. Rallis, C., Del Buono, J. & Logan, M. P. Tbx3 can alter limb position along the rostrocaudal axis of the developing embryo. Development 132, 1961–1970 (2005).

62. Laufer, E., Nelson, C. E., Johnson, R. L., Morgan, B. A. & Tabin, C. Sonic hedgehog and Fgf-4 act through a signaling cascade and feedback loop to integrate growth and patterning of the developing limb bud. Cell 79, 993–1003 (1994). 54.

63. Niswander, L., Jeffrey, S., Martin, G. R. & Tickle, C. A positive feedback loop coordinates growth and patterning in the vertebrate limb. Nature 371, 609–612 (1994).

64. Michos, O. et al. Gremlin-mediated BMP antagonism induces the epithelial–mesenchymal feedback signaling controlling metanephric kidney and limb organogenesis. Development 131, 3401–3410 (2004).

65. Logan, Malcolm, James F. Martin, Andras Nagy, Corrinne Lobe, Eric N. Olson, and Clifford J. Tabin. "Expression of Cre Recombinase in the Developing Mouse Limb Bud Driven by A Prxl Enhancer." Genesis 33.2 (2002): 77-80.

66. Lu, P., Y. Yu, Y. Perdue, and Z. Werb. "The Apical Ectodermal Ridge Is a Timer for Generating Distal Limb Progenitors." Development 135.8 (2008): 1395-405.